Leaf-level photosynthetic capacity in lowland Amazonian and high-elevation Andean tropical moist forests of Peru

Nur H. A. Bahar[1], F. Yoko Ishida[2], Lasantha K. Weerasinghe[1,3], Rossella Guerrieri[4,5], Odhran S. O'Sullivan[1], Keith J. Bloomfield[1], Gregory P. Asner[6], Roberta E. Martin[6], Jon Lloyd[2,7], Yadvinder Malhi[8], Oliver L. Phillips[9], Patrick Meir[1,5], Norma Salinas[8,10], Eric G. Cosio[10], Tomas F. Domingues[11], Carlos A. Quesada[12], Felipe Sinca[6], Alberto Escudero Vega[10], Paola P. Zuloaga Ccorimanya[13], Jhon del Aguila-Pasquel[14,15], Katherine Quispe Huaypar[13], Israel Cuba Torres[13], Rosalbina Butrón Loayza[16], Yulina Pelaez Tapia[13], Judit Huaman Ovalle[13], Benedict M. Long[1,17], John R. Evans[1,17] and Owen K. Atkin[1,18]

[1]Division of Plant Sciences, Research School of Biology, The Australian National University, Canberra, ACT 2601, Australia; [2]Centre for Tropical Environmental and Sustainability Science, College of Marine and Environmental Sciences, James Cook University, Cairns, Qld, Australia; [3]Faculty of Agriculture, University of Peradeniya, Peradeniya 20400, Sri Lanka; [4]Centre for Ecological Research and Forestry Applications (CREAF), Universidad Autonoma de Barcelona, Edificio C, 08290 Cerdanyola, Barcelona Spain; [5]School of Geosciences, University of Edinburgh, Edinburgh, EH9 3JN, UK; [6]Department of Global Ecology, Carnegie Institution for Science, Stanford, CA 94305, USA; [7]Department of Life Sciences, Imperial College London, Silwood Park Campus, Ascot, SL5 7PY, UK; [8]Environmental Change Institute, School of Geography and the Environment, University of Oxford, South Parks Road, Oxford, OX1 3QY, UK; [9]School of Geography, University of Leeds, Woodhouse Lane, Leeds, LS9 2JT, UK; [10]Seccion Quimica, Pontificia Universidad Católica del Perú, Av Universitaria 1801, San Miguel, Lima, Perú; [11]Faculdade de Filosofia Ciências e Letras de Ribeirão Preto, Universidade de São Paulo, Sao Paulo, Brazil; [12]Instituto Nacional de Pesquisas da Amazonia (INPA), Manaus, Brazil; [13]Escuela Profesional de Biologia, Universidad Nacional de San Antonio Abad del Cusco, Av de la Cultura, No. 733, Cusco, Perú; [14]Instituto de Investigaciones de la Amazonia Peruana (IIAP), Av. José A. Quiñones km. 2.5, Apartado Postal 784, Iquitos, Perú; [15]School of Forest Resources and Environmental Science, Michigan Technological University, 1400 Townsend Drive, Houghton, MI 49931, USA; [16]Museo de Historia Natural, Universidad Nacional de San Antonio Abad del Cusco, Av de la Cultura, No. 733, Cusco, Perú; [17]ARC Centre of Excellence for Translational Photosynthesis, Research School of Biology, The Australian National University, Building 134, Canberra, ACT 2601, Australia; [18]ARC Centre of Excellence in Plant Energy Biology, Research School of Biology, The Australian National University, Building 134, Canberra, ACT 2601, Australia

Author for correspondence:
Owen K. Atkin
Tel: +61 (0)2 6125 5046
Email: Owen.Atkin@anu.edu.au

Received: *3 November 2015*
Accepted: *23 May 2016*

New Phytologist (2016)
doi: 10.1111/nph.14079

Key words: carboxylation capacity, elevation, leaf traits, nitrogen (N), phosphorus (P), ribulose bisphosphate regeneration, temperature, tropical forests.

Summary

- We examined whether variations in photosynthetic capacity are linked to variations in the environment and/or associated leaf traits for tropical moist forests (TMFs) in the Andes/western Amazon regions of Peru.
- We compared photosynthetic capacity (maximal rate of carboxylation of Rubisco (V_{cmax}), and the maximum rate of electron transport (J_{max})), leaf mass, nitrogen (N) and phosphorus (P) per unit leaf area (M_a, N_a and P_a, respectively), and chlorophyll from 210 species at 18 field sites along a 3300-m elevation gradient. Western blots were used to quantify the abundance of the CO_2-fixing enzyme Rubisco.
- Area- and N-based rates of photosynthetic capacity at 25°C were higher in upland than lowland TMFs, underpinned by greater investment of N in photosynthesis in high-elevation trees. Soil [P] and leaf P_a were key explanatory factors for models of area-based V_{cmax} and J_{max} but did not account for variations in photosynthetic N-use efficiency. At any given N_a and P_a, the fraction of N allocated to photosynthesis was higher in upland than lowland species. For a small subset of lowland TMF trees examined, a substantial fraction of Rubisco was inactive.
- These results highlight the importance of soil- and leaf-P in defining the photosynthetic capacity of TMFs, with variations in N allocation and Rubisco activation state further influencing photosynthetic rates and N-use efficiency of these critically important forests.

Introduction

Tropical moist forests (TMFs) play a significant role in the terrestrial carbon cycle, contributing one-third of global gross primary productivity (Beer *et al.*, 2010; Malhi, 2010). Understanding the factors that regulate leaf photosynthesis (A) in TMFs is a prerequisite for modelling carbon storage in tropical ecosystems, with A being influenced *inter alia* by nutrient supply [particularly nitrogen (N) and phosphorus (P)], elevation and growth temperature.

Early studies in lowland TMFs implicated low foliar P concentrations as a major influence on light-saturated net photosynthesis

(A_{sat}) (Reich & Walters, 1994; Raaimakers *et al.*, 1995), with soil P being a major factor limiting Amazon productivity (Quesada *et al.*, 2012). Foliar P is crucial to the fine-tuning of A_{sat} (Fredeen *et al.*, 1989; Jacob & Lawlor, 1993) via regulation of key intermediates in carbon metabolism (e.g. ATP, NADPH and sugar phosphates including ribulose 1,5-bisphosphate (RuBP)). While the direct effect of P limitation is primarily on RuBP regeneration, reductions in Rubisco activity also occur (Brooks, 1986; Jacob & Lawlor, 1992; Loustau *et al.*, 1999). Although Meir *et al.* (2002, 2007) and Reich *et al.* (2009) showed that A_{sat} at a given leaf N concentration ([N]) was lower in lowland tropical trees than in their temperate counterparts, the extent to which P limitations *per se* alter $A_{sat} \leftrightarrow$ [N] relations within TMFs is uncertain (Bloomfield *et al.*, 2014a; Domingues *et al.*, 2015). A further unknown is the extent to which large elevation gradients affect $A_{sat} \leftrightarrow$ [N] relations in the tropics. Upland TMFs are more likely to be limited by N than their lowland counterparts (Tanner *et al.*, 1998). Upland TMFs also experience lower temperatures and atmospheric CO_2 partial pressures, more frequent cloud cover and greater leaf wetness (Grubb, 1977; Vitousek, 1984; Girardin *et al.*, 2010; Bruijnzeel *et al.*, 2011). Such factors can limit A_{sat} (Terashima *et al.*, 1995; Bruijnzeel & Veneklaas, 1998; Letts & Mulligan, 2005), leading to declines in productivity (Girardin *et al.*, 2010). A_{sat} values in upland TMFs have been documented (e.g. Quilici & Medina, 1998; Cordell *et al.*, 1999; Hikosaka *et al.*, 2002; Letts & Mulligan, 2005; Rada *et al.*, 2009), showing A_{sat} to be constant with increasing elevation (Cordell *et al.*, 1999), or declining with increasing elevation (Hikosaka *et al.*, 2002; Wittich *et al.*, 2012).

Rates of A_{sat} are subject to variations in stomatal conductance (g_s) and the partial pressure of internal leaf CO_2 (C_i) (Santiago & Mulkey, 2003). As variations in C_i alter both CO_2 uptake and photorespiratory CO_2 release, variations in C_i could potentially confound our understanding of how environmental gradients alter N investment in *A*. By contrast, variations in g_s have less impact on the fundamental, biochemical parameter of photosynthetic capacity – that being the maximum rate of carboxylation by Rubisco (i.e. V_{cmax}). Positive correlations between V_{cmax} and leaf [N] have been reported for some tropical species (Carswell *et al.*, 2000; Meir *et al.*, 2002, 2007; Domingues *et al.*, 2005; Kumagai *et al.*, 2006; Vårhammar *et al.*, 2015), whereas in others no strong $V_{cmax} \leftrightarrow$ [N] relationship was observed (Coste *et al.*, 2005; van de Weg *et al.*, 2012; Dusenge *et al.*, 2015). Although reports on V_{cmax} are less widespread in the tropics than those on A_{sat}, the available data suggest that V_{cmax} values, as well as V_{cmax} per unit N (herein termed '$V_{cmax,N}$'), are lower in lowland TMFs than in their nontropical counterparts (Carswell *et al.*, 2000; Meir *et al.*, 2002, 2007; Domingues *et al.*, 2007, 2010; Walker *et al.*, 2014; Vårhammar *et al.*, 2015). Kattge *et al.* (2009) re-analysed data to show that V_{cmax} per unit N in TMFs growing on young, relatively high nutrient status soils was higher compared with their older, Ferralsol and Acrisol soil counterparts which are characterized by very low soil P availability (Quesada *et al.*, 2010). These observations are consistent with laboratory studies showing reduced V_{cmax} (Lauer *et al.*, 1989; Loustau *et al.*, 1999) and reduced N allocation to Rubisco (Warren & Adams, 2002) under P-limited conditions. Increased allocation of N to nonphotosynthetic components may also play a role (Domingues *et al.*, 2010; Lloyd *et al.*, 2013), as might inactivation of Rubisco (Stitt & Schulze, 1994). Yet, doubt remains regarding the general $V_{cmax} \leftrightarrow$ [N] relationship in TMFs because of the scarcity of data, in both lowland and upland TMFs. Comprehensive surveys of V_{cmax} (and the maximum rate of electron transport (J_{max})) across lowland and upland TMFs are required to establish whether there are generalized patterns of photosynthetic capacity in relation to environmental conditions and/or other leaf traits.

TMF species with higher leaf nutrient concentrations and lower leaf mass per unit leaf area (M_a) values are often found in more fertile soils (Fyllas *et al.*, 2009), and M_a tends to increase with increasing elevation (Hikosaka *et al.*, 2002; van de Weg *et al.*, 2009; Almeida *et al.*, 2012; Asner *et al.*, 2014b); leaf chemistry also systematically shifts along elevation gradients in the tropics (Asner *et al.*, 2014b). Large variations in leaf traits have also been observed among co-occurring species, reflecting the importance of phylogenetic relationships in determining trait values in TMFs (Townsend *et al.*, 2007; Kraft *et al.*, 2008; Fyllas *et al.*, 2009). Whether similar patterns hold for estimates of V_{cmax} in lowland and upland TMFs (and $V_{cmax,N}$), is, however, not known.

Variations in $V_{cmax,N}$ underlie variations in photosynthetic N-use efficiency. Further insights can be gained by quantifying the proportion of N allocated to the pigment–protein complexes (n_P), electron transport (n_E) and Rubisco (n_R) (Evans & Seemann, 1989; Pons *et al.*, 1994; Hikosaka, 2004). Quantification of V_{cmax}, J_{max}, leaf chlorophyll and [N] can be used to estimate n_P, n_E and n_R (Evans & Seemann, 1989; Niinemets & Tenhunen, 1997). In nontropical plants, lower A_{sat} at a given N (A_N) is associated with reduced allocation of N to photosynthesis and increased allocation to nonphotosynthetic components (Poorter & Evans, 1998; Westbeek *et al.*, 1999; Warren & Adams, 2001; Takashima *et al.*, 2004; Hikosaka & Shigeno, 2009). Similarly, variations in A_N were associated with differences in N allocation to and within the photosynthetic apparatus in glasshouse-grown tropical tree seedlings (Coste *et al.*, 2005) and in high-elevation TMFs of Rwanda (Dusenge *et al.*, 2015). To our knowledge, no study has quantified N allocation patterns in field-grown tropical trees, and not with respect to field sites in upland and lowland TMFs.

We examined variations in photosynthetic capacity and leaf traits across TMF canopies located at 18 sites along a 3300-m elevation gradient stretching from lowland western Amazonia to the Andean tree line in Peru. The study included 11 lowland sites in northern and southern Peru (elevation 117–223 m above sea level (asl)), and seven upland sites at elevations of 1527–3379 m asl in southern Peru. Our site selection enabled an assessment of the potential role of P availability on photosynthetic performance across Amazonian–Andean TMF sites differing > 40-fold in total soil P. The upland sites were characterized by a floristically distinct assemblage of montane forest species, with the transition

from lowland moist forests to upland montane forests coinciding with an increase in cloud cover (van de Weg *et al.*, 2009; Bruijnzeel *et al.*, 2011). In conjunction with the recent findings of the key role of P in modulating carbon investment (Quesada *et al.*, 2012) and photosynthesis (Bloomfield *et al.*, 2014b) of tropical trees, and that leaf P varies predictably along soil P and elevation gradients (Asner *et al.*, 2014b), we addressed the following questions: do tropical TMF species growing on low-P soils exhibit lower photosynthetic capacity and photosynthetic N-use efficiency than TMF trees growing on sites with higher P availability? Are there marked differences in V_{cmax}, J_{max} and $V_{cmax,N}$ between lowland Amazonian and upland Andean TMFs? Are differences in V_{cmax}, J_{max} and $V_{cmax,N}$ linked to concomitant variations in other leaf traits and/or environmental variables?

Materials and Methods

Study sites

Field work was carried out in 18 one-hectare long-term monitoring plots in Peru which contribute to the ABERG and RAINFOR networks of permanent sample plots. The plots are arrayed along gradients of elevation (117–3379 m asl) and soil nutrient status (Table 1). For each site, climate data were obtained from Asner *et al.* (2014a) and Y. Malhi (unpublished). Marked changes in species richness, canopy cover and tree height occur along the elevation gradient (Asner *et al.*, 2014a; Girardin *et al.*, 2014b; Silman, 2014), reflecting local geological substrates, as well as changes in growth temperature, cloud cover and light environment. In addition to marked inter-site differences in total soil [N] (0.6–15.5 g N kg^{-1}), substantial variation in total soil [P] occurs across both the lowland (38–727 mg P kg^{-1}) and upland sites (496–1631 mg P kg^{-1}) (Table 1). Soils at three of the lowland sites in northern Peru (JEN-12, ALP-30 and ALP-40) are notable for being low nutrient status arenosols/podzols ('white sands'). Among the lowland and upland sites, mean annual precipitation (MAP) values range from 1560 to 5300 mm yr^{-1}. Mean annual temperature ranged from 8.0 to 18.8°C across the upland sites, and 24.4 to 26.6°C among the lowland sites.

At each site, tree climbers collected upper canopy branches (supporting leaves considered to be typically exposed to full sunlight for much of the day) from dominant tree species. There was little replication of individual species possible at any site. Each tree was initially identified to the genus level and, whenever possible, to the species level. A total of 353 individual trees drawn from 210 species were sampled across the 18 sites. See Supporting Information Methods S1 for further details.

Leaf gas exchange measurements

Measurements of leaf gas exchange were made during July to September 2011, using portable photosynthesis systems (Li-Cor 6400XT infrared gas analyser; Li-Cor BioSciences, Lincoln, NE, USA). Measurements were made on the most recently fully expanded leaves attached to the cut branches (which had been recut under water immediately after harvesting to preserve xylem water continuity).

CO_2 response curves of light-saturated photosynthesis ($A \leftrightarrow C_i$ curves) (at 1800 μmol photons m^{-2} s^{-1}) were obtained within 30–60 min after branch detachment. CO_2 concentrations inside the reference chamber ranged in a stepped sequence from 35 to 2000 μmol mol^{-1} (see Methods S2 for details). Block temperatures within the chamber were set to the prevailing daytime air temperature at each site (from 25 to 28°C). The resultant $A \leftrightarrow C_i$ curves (examples shown in Fig. 1) were fitted following the model described by Farquhar *et al.* (1980) in order to calculate V_{cmax} and J_{max} on a leaf area basis; see Methods S2 for details. For every $A \leftrightarrow C_i$ curve, recorded air pressure was used to correct for altitudinal changes in O_2 partial pressure, and to calculate intercellular CO_2 (C_i) values on a partial pressure basis.

Rates of CO_2 exchange were corrected for possible gas diffusion through the gasket of the Li-Cor 6400XT leaf chamber (Bruhn *et al.*, 2002) before calculation of V_{cmax} and J_{max}. Assuming infinite internal diffusion conductance (g_m), Michaelis constants of Rubisco for CO_2 (K_c) and O_2 (K_o) at a reference temperature of 25°C were assumed to be 40.4 Pa and 24.8 kPa, respectively (von Caemmerer *et al.*, 1994); these values were adjusted to actual leaf temperatures assuming activation energies of 59.4 and 36 kJ mol^{-1} for K_c and K_o, respectively (Farquhar *et al.*, 1980). Fitted parameters were then scaled to a reference temperature of 25°C using activation energies of 64.8 and 37.0 kJ mol^{-1} for V_{cmax} and J_{max}, respectively (Farquhar *et al.*, 1980). Finally, rates of A obtained at ambient CO_2 concentrations of 400 and 2000 μmol mol^{-1} (A_{400} and A_{2000}, respectively) were extracted from the $A \leftrightarrow C_i$ curves and reported separately.

As atmospheric CO_2 was not always saturating for measurements of upland species (because of low atmospheric partial pressure, resulting in insufficient CO_2-saturated rates of A to enable calculation of J_{max}), it was likely that J_{max} may have been underestimated in some cases; where this was likely to be the case (i.e. where there was no clear plateauing of A at high C_i values), we excluded the resultant J_{max} values from the Andean data set. With the exception of a few cases (e.g. *Schefflera* sp.; Fig. 1), $A \leftrightarrow C_i$ curves typically flattened out at high C_i values (> 90% of curves), with A increasing slightly as C_i values increased further (see Fig. 1), suggesting that feedback inhibition of A through limitations in triose-phosphate utilization (TPU) was unlikely.

Leaf structure and chemistry determination

Leaves were collected immediately following the gas exchange measurements. Initially, the leaf mid rib was removed; thereafter, a digital photograph was taken using a high-resolution scanner (CanoScan LiDE 210; Canon, Hanoi, Vietnam) and later analysed for leaf area (ImageJ, v.1.38; National Institutes of Health (NIH), USA). Leaves were then placed in an oven at 70°C for at least 48 h, the dry mass was measured and the leaf mass per unit leaf area (M_a) was calculated. Total leaf N and P concentrations in dried leaves were determined using the Kjeldahl acid digest method, as detailed in Ayub *et al.* (2011).

New Phytologist (2016)
www.newphytologist.com

Table 1 Description of the sampled Peruvian field sites

Category	Site code	Latitude	Longitude	Elevation (m asl)	No. of species	MAT (°C)	MAP (m)	Atm. Pressure (kPa)	Soil classification	Total soil nutrients		Leaf chemistry			
										[N] ($g\,kg^{-1}$)	[P] ($mg\,kg^{-1}$)	Leaf N_a ($g\,m^{-2}$)	Leaf P_a ($g\,m^{-2}$)	Leaf N : P	M_a ($g\,m^{-2}$)
Lowland	SUC-05	−3.2558	−72.8942	132	20	26.2	2.75	100	Alisols	1.9	276	1.94 ± 0.61	0.06 ± 0.04	30.1 ± 7.03	129 ± 31
	TAM-05	−12.8309	−69.2705	223	8	24.4	1.90	99	Cambisols	1.6	256	2.14 ± 0.27	0.08 ± 0.02	28.6 ± 9.49	119 ± 27
	JEN-11	−4.8781	−73.6295	131	18	26.6	2.70	100	Acrisols	1.8	141	2.12 ± 0.52	0.06 ± 0.02	27.9 ± 10.4	144 ± 37
	ALP-01	−3.9500	−73.4333	120	18	25.2	2.69	100	Gleysols	0.6	110	1.90 ± 0.40	0.08 ± 0.03	26.2 ± 8.62	119 ± 24
	SUC-01	−3.2519	−72.9078	117	17	26.2	2.75	100	Plinthosols	1.7	305	1.81 ± 0.63	0.09 ± 0.03	22.1 ± 4.99	123 ± 27
	JEN-12	−4.8990	−73.6276	135	19	26.6	2.70	100	Podzols	6.9	133	1.97 ± 0.52	0.09 ± 0.05	21.9 ± 10.42	156 ± 31
	ALP-30	−3.9543	−73.4267	150	21	25.2	2.69	100	Arenosols	0.8	38	1.67 ± 0.47	0.09 ± 0.04	20.8 ± 6.85	145 ± 46
	CUZ-03	−12.5344	−69.0539	205	12	24.4	1.90	99	Cambisols	2.4	727	1.88 ± 0.47	0.10 ± 0.04	17.2 ± 5.97	109 ± 18
	ALP-40	−3.9410	−73.4400	142	12	26.3	2.76	100	Podzols	2.1	59	1.84 ± 0.36	0.10 ± 0.02	16.8 ± 5.00	171 ± 50
	TAM-09	−12.8309	−69.2843	219	13	24.4	1.90	99	Alisols	1.1	326	2.19 ± 0.45	0.14 ± 0.03	16.4 ± 3.77	105 ± 21
	TAM-06	−12.8385	−69.2960	215	13	24.4	1.90	99	Alisols	1.7	529	2.56 ± 0.34	0.17 ± 0.04	15.3 ± 2.84	126 ± 26
Upland	SPD-02	−13.0491	−71.5365	1527	19	18.8	5.30	83	Cambisols	8.8	1631	2.23 ± 0.45	0.16 ± 0.05	15.4 ± 4.05	126 ± 36
	SPD-01	−13.0475	−71.5423	1776	21	17.4	5.30	85	Cambisols	11.9	1071	2.25 ± 0.35	0.16 ± 0.04	14.3 ± 3.34	124 ± 29
	TRU-08	−13.0702	−71.5559	1885	20	18.0	2.47	82	Cambisols	8.1	496	1.99 ± 0.36	0.12 ± 0.05	16.9 ± 3.54	165 ± 38
	ESP-01	−13.1751	−71.5948	2863	17	13.1	1.56	72	Umbrisols	14.8	981	2.39 ± 0.50	0.19 ± 0.05	12.7 ± 1.78	140 ± 32
	TRU-03	−13.1097	−71.5995	3044	13	11.8	1.78	71	Umbrisols	15.5	787	2.24 ± 0.44	0.21 ± 0.04	10.5 ± 2.35	164 ± 40
	WAQ-01	−13.1908	−71.5874	3045	13	11.8	1.56	72	Umbrisols	8.8	1414	2.68 ± 0.42	0.24 ± 0.05	11.5 ± 2.16	149 ± 46
	TRU-01	−13.1136	−71.6069	3379	16	8.0	1.98	67	Umbrisols	15.0	856	2.53 ± 0.31	0.21 ± 0.04	11.2 ± 3.10	151 ± 49

Lowland sites are listed in order of decreasing leaf nitrogen (N) : phosphorus (P) ratios, while upland sites are listed in order of increasing elevation. Extremely low soil P did not necessarily produce low leaf P as in the case of ALP-03 and ALP-04, and therefore lowland sites were ranked according to the leaf N to P ratio, which provides a better indication of nutrient limitation (Aerts & Chapin, 2000). Atmospheric pressure was obtained from a Li-Cor 6400XT gas exchange system. For each site, a site code is shown as designated by the Joint Amazon Carnegie RAINFOR Expedition (JACARE); values of total soil N and P are shown (expressed per unit soil dry mass). Also shown are average leaf area-based concentrations of total nitrogen (N_a) and phosphorus (P_a), as well as the ratio of leaf N : P and leaf mass per unit area (M_a), all shown with SD. Soil classification follows the World Reference Base (WRB). asl, above sea level; MAP, mean annual precipitation; MAT, mean annual temperature. Sources: Asner *et al.* (2014a), Quesada *et al.* (2010; pers. comm.) and Y. Malhi (unpublished).

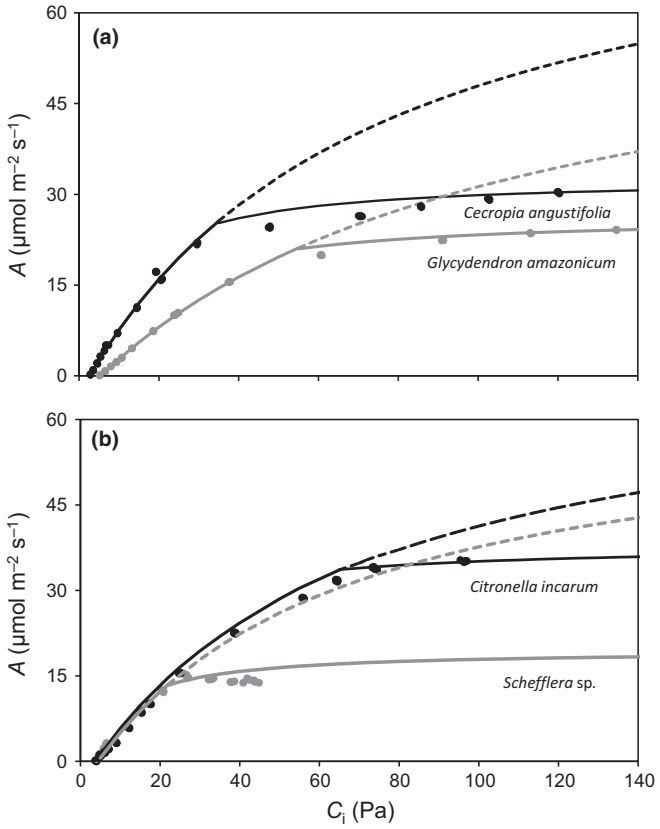

Fig. 1 Fitted curves of the response of CO_2 assimilation rate (*A* (area-based)) to intercellular CO_2 (C_i) at saturating light for (a) a lowland species *Glycydendron amazonicum* (TAM-09) and an upland species *Cecropia angustifolia* (SPD-01) and (b) two upland species, *Citronella incarum* (TRU-03) and *Schefflera* sp. (WAQ-01). Closed circles are the measured rates of assimilation, *A*. Solid lines correspond to fitted response and dashed lines correspond to estimated response at high C_i. The maximum Rubisco carboxylation capacity (V_{cmax}) was calculated from the curvature of the dashed line and the maximum electron transport rate (J_{max}) was calculated from the points where *A* saturated. Individual leaves were measured at temperatures set close to the prevailing growth temperature, and therefore V_{cmax} and J_{max} were then normalized to 25°C. CO_2 was not always saturating for most upland measurements because of low partial pressure and/or phosphate limitation.

Chlorophyll and Rubisco measurements

Leaf discs from mature leaves adjacent to the gas exchange leaf were collected and transferred to a −80°C cryogenic field container for subsequent chlorophyll and Rubisco assays in the laboratory.

The chlorophyll content of each set of leaf discs was determined using a dual-beam scanning UV-VIS spectrometer (Lambda 25; Perkin-Elmer, Shelton, CT, USA) after extraction of chlorophyll pigments from two frozen leaf discs (0.77 cm^2 each) with 100% acetone and $MgCO_3$, as outlined in Asner *et al.* (2014b). Chlorophyll *a*: *b* ratios varied between 2.45 and 2.75, which is consistent with results of past studies on tropical trees in the Peruvian Amazon (Asner & Martin, 2011).

Protein was extracted from frozen leaf discs following the method outlined in Gaspar *et al.* (1997) with slight modifications (see Methods S3 for details of optimization of protein assays). Frozen samples of 0.50 cm^2 were ground in Eppendorf tubes and washed consecutively in 100% methanol, hexane and acetone. Treated leaf powder was then resuspended in protein extraction buffer (140 mM Tris base, 105 mM Tris–HCl, 0.5 mM ethylenediaminetetraacetic acid, 2% lithium dodecyl sulfate (LDS) and 10% glycerol) containing 5 mM DTT and protease inhibitor cocktail (Sigma-Aldrich, Castle Hill, NSW, Australia), heated for 10 min at 100°C to completely dissolve extracted protein, then clarified by centrifugation (14 000 ***g***; 10 min; room temperature). The supernatant was tested for protein content.

Equivalent volumes of supernatant were diluted in 4× SDS-PAGE sample buffer (Invitrogen Life Technologies, Carlsbad, CA, USA) then loaded onto gels. As we extracted protein from a known amount of leaf area, we were able to analyse our samples on an equivalent leaf area basis. Varying concentrations of Rubisco, purified from tobacco (*Nicotiana tabacum*), were also loaded onto gels, serving as a calibration series. Proteins were run on 4–12% NuPAGE Bis-Tris gels (Invitrogen Life Technologies) according to the manufacturer's instructions and transferred to Immobilon-P PVDF membranes (Merck Millipore, Kilsyth, Vic., Australia) using an XCell II Blot module (Invitrogen). Membranes were blocked with 5% skimmed milk powder in Tris-buffered saline containing 0.5% Tween-20 (TBS-T) and an antibody raised in rabbits against tobacco Rubisco (used at 1 : 5000) prepared by Spencer Whitney (Research School of Biology, Australian National University, Canberra). Secondary antibody (goat-anti-rabbit-alkaline phosphatase conjugate; Agrisera, Vannas, Sweden) was diluted 1 : 5000. Blots were visualized using the Attophos AP fluorescent substrate system (Promega, Madison, WI, USA) and imaged using a Versa-Doc (Bio-Rad, Hercules, CA, USA) imaging system. Blots were analysed using Quantity One software (Bio-Rad) and the relative band densities of each protein were determined from duplicate samples, and data averaged. The Rubisco concentration was calculated from the large subunit (molecular mass of 55 kD and 16% N by weight).

Estimation of N allocation in photosynthetic metabolism

N allocation in three major photosynthetic components (pigment–protein complexes, electron transport and Rubisco) for all leaves was estimated from chlorophyll concentration, V_{cmax} and J_{max}, respectively. N allocation to pigment–protein complexes (n_P) was calculated by assuming 44 mol N per mol of chlorophyll (Evans, 1989). N allocation to Rubisco (n_R) was estimated from values of V_{cmax} according to Harrison *et al.* (2009), with slight modification (2.33 mol CO_2 (mol Rubisco sites)$^{-1}$ s^{-1} for the catalytic turnover number of Rubisco at 25°C; Harrison *et al.*, 2009). We here assumed that all Rubisco was fully activated and mesophyll conductance was infinite. The allocation of N to electron transport components (n_E) was calculated from J_{max} assuming 160 mol electrons (mol cytochrome f)$^{-1}$ s^{-1} and 8.85 mol N (mmol cytochrome f)$^{-1}$ (Evans & Seemann, 1989). The proportion of total leaf N allocated to each photosynthetic

component was calculated by dividing the N investment in each component by the total N content per unit leaf area.

Data analysis

Log_{10} transformations were carried out on leaf trait values when necessary to ensure normality and minimize heterogeneity of residuals. Student *t*-tests (two-tailed) were used to compare overall means of lowland and upland species. Standardized major axis (SMA) estimation was used to describe the best-fit relationship between pairs of variables and to assess whether relationships differed between lowland and upland elevation classes, using SMATR version 2.0 software (Falster *et al.*, 2006; Warton *et al.*, 2006). The decision to compare upland and lowland trait relationships reflects the strong elevation contrast in environments, phylogeny, floristic composition and forest structure (Gentry, 1988; van de Weg *et al.*, 2009; Asner *et al.*, 2014b). The significance of SMA regression was tested at $\alpha = 0.05$.

In addition to the above bivariate analyses, we also used a mixed-effects linear model combining fixed and random components (Pinheiro & Bates, 2000) to account for variability in area- and N-based rates of V_{cmax}, and area-based rates of J_{max}. This approach enabled the structured nature of the data set to be recognized, and for interactions between multiple terms to be considered. The model's fixed effect included continuous explanatory variables only: leaf traits (M_a, and area-based leaf N and P), and environment variables (soil P and N concentrations, mean annual temperature (MAT) and the effective cation exchange capacity of soil (ECEC)). Model specification and validation were based on the protocols outlined in Zuur *et al.* (2009) and fitted using the *nlme* package (R package v.3.1-105; R Foundation for Statistical Computing, Vienna, Austria; R Development Core Team, 2011). Details of the model selection process are provided in Table S6. Briefly, phylogeny (family/genus/species) was treated as a nested random effect, placing focus on the variation contained within these taxonomic terms, rather than mean values for each level. Site variation was captured by soil and environmental factors considered in the model's fixed component; because of this, no site term was included in the random component. Model comparisons and the significance of fixed-effects terms were assessed using Akaike's information criterion (AIC). Unless otherwise stated, statistical analysis was performed using SPSS v.20 (IBM Corporation, Armonk, NY, USA).

Results

Variations in leaf chemistry and structure

Among lowland sites, there was a six-fold variation in leaf N : P ratios (7.6–45.9) (Table S1), but for upland sites, when ranked according to increasing elevation, mean values of leaf N : P were largely consistent across sites of similar elevation (Table 1). Across all sites (lowland and upland combined), variations in leaf N : P ratios were predominantly driven by variations in leaf [P] ($r^2 = 0.59$; $P < 0.01$; Table S2) rather than leaf [N]. Variations in area-based leaf [P] (P_a) were positively correlated with soil [P] ($r^2 = 0.37$; $P < 0.01$) and elevation ($r^2 = 0.48$; $P < 0.01$). Weaker positive associations were observed for area-based leaf [N] (N_a) with total soil [N] ($r^2 = 0.10$; $P < 0.01$) and elevation ($r^2 = 0.14$; $P < 0.01$).

Leaf mass per unit leaf area (M_a) varied widely, both among and within lowland (54–230 g m^{-2}) and upland (60–249 g m^{-2}) sites (Tables 1, S1). Although variations in M_a were not correlated with variations in soil [P], there were significant (but weak) correlations between M_a and total soil [N] ($r^2 = 0.04$; $P < 0.01$) and elevation ($r^2 = 0.03$; $P < 0.01$) (Table S2). The overall mean of M_a for the sampled upland species (143 ± 39 g m^{-2}) was significantly higher than that of the lowland species (132 ± 35 g m^{-2}; Table 2, $P < 0.05$).

Across all 18 sites, leaf N_a was positively correlated with M_a ($P < 0.01$; $r^2 = 0.12$; Table S2), with the $N_a \leftrightarrow M_a$ relationship being stronger among upland than lowland sites ($r^2 = 0.07$ for lowland sites and $r^2 = 0.20$ for upland; see Table S3 for *P*-values, slopes and intercepts of each SMA relationship). The slope and intercept of the relationship differed between the two elevation classes (Fig. 2a) – upland species exhibited higher N_a for a given M_a than lowland species, particularly in low M_a species. Across all sites, leaf P_a exhibited a weak, positive correlation with M_a ($P < 0.01$; $r^2 = 0.04$; Table S2). Similarly, a weak positive $P_a \leftrightarrow M_a$ relationship ($P = 0.003$; $r^2 = 0.04$; Table S3) was found among upland species (Fig 2b). Although no significant $P_a \leftrightarrow M_a$ relationship was found among lowland species (with leaf P_a varying 20-fold; Table S1), mean values of P_a at a given M_a were lower than those of their upland counterparts.

Variations in photosynthetic metabolism

Light-saturated rates of photosynthesis per unit leaf area, measured at the prevailing daytime air temperature (T) at each site and at an atmospheric CO_2 concentration of 400 μmol mol^{-1} ($A_{400,a}$), differed among co-occurring species (Table S1). However, there was no significant difference between mean values of $A_{400,a}$ from lowland and upland classes (Table 2). This uniformity of $A_{400,a}$ occurred despite significantly lower measuring T values at the high-elevation sites (overall means: lowland 29.4 ± 0.9°C; upland 25.7 ± 2.1°C; $P < 0.05$) and lower intercellular CO_2 partial pressure (C_i) (overall means: lowland 28.4 ± 3.7 Pa; upland 18.8 ± 3.0 Pa; $P < 0.05$) (Table S4). Assessed on a per unit leaf N basis ($A_{400,N}$), average rates were lower at the upland sites compared with their lowland counterparts (Tables 2, S4), reflecting higher leaf N_a for trees at high elevation (Table 1). Across sites, mean $A_{400,N}$ decreased with decreasing MAT (Fig. S1d). Area-based rates of photosynthesis at elevated CO_2 ($A_{2000,a}$) were higher in upland (17.1–26.5 μmol m^{-2} s^{-1}; Table S4) than lowland (16.1–22.6 μmol m^{-2} s^{-1}) species ($P < 0.05$). The higher values of $A_{2000,a}$ at the upland sites were achieved despite the colder temperatures. On a per unit leaf N basis ($A_{2000,N}$), average rates were similar for the two elevation classifications (Table S4; Fig. S1e).

To explore differences in the rates of the underlying components of net photosynthesis, we compared maximal area-based rates of CO_2 fixation by Rubisco ($V_{cmax,a}$) and photosynthetic

Table 2 Mean values and standard deviation of leaf traits for upland and lowland species

Leaf traits	Leaf N_a ($g\,m^{-2}$)	Leaf P_a ($g\,m^{-2}$)	Leaf N : P	M_a ($g\,m^{-2}$)	$A_{400,a}$ ($\mu mol\ m^{-2}\ s^{-1}$)	$A_{400,N}$ ($\mu mol\ gN^{-1}\ s^{-1}$)	$V_{cmax,a}^{25}$ ($\mu mol\ m^{-2}\ s^{-1}$)	$J_{max,a}^{25}$ ($\mu mol\ m^{-2}\ s^{-1}$)	$J_{max,a}^{25}$: $V_{cmax,a}^{25}$	$V_{cmax,N}^{25}$ ($\mu mol\ gN^{-1}\ s^{-1}$)	n_A	n_P	n_R	n_E
Lowland species	1.96 ± 0.52^a	0.09 ± 0.05^a	22.2 ± 8.6^a	132 ± 35^a	8.2 ± 3.9^a	4.3 ± 2.2^a	35.9 ± 14.6^a	66.7 ± 18.6^a	1.86 ± 0.40^a	18.9 ± 8.1^a	0.37 ± 0.11^a	0.24 ± 0.09^a	0.09 ± 0.04^a	0.03 ± 0.01^a
Upland species	2.31 ± 0.44^b	0.18 ± 0.06^b	13.5 ± 3.6^b	143 ± 39^b	7.6 ± 3.6^a	3.4 ± 1.7^b	48.8 ± 20.0^b	96.9 ± 36.9^b	1.92 ± 0.36^a	22.5 ± 9.4^b	0.38 ± 0.08^a	0.22 ± 0.07^a	0.11 ± 0.04^b	0.03 ± 0.01^b

Values are expressed on an area basis. Leaf N_a, leaf nitrogen; leaf P_a, leaf phosphorus; leaf N : P, leaf nitrogen to phosphorus ratio; M_a, leaf mass per unit leaf area; $A_{400,a}$, area-based light-saturated net photosynthesis measured at 400 $\mu mol\ mol^{-1}$ atmospheric [CO_2]; $A_{400,N}$, area-based light-saturated net photosynthesis measured at 400 $\mu mol\ mol^{-1}$ atmospheric [CO_2] per unit leaf nitrogen; $V_{cmax,a}^{25}$, maximum carboxylation velocity of Rubisco normalized to 25°C; $J_{max,a}^{25}$, maximum rate of electron transport normalized to 25°C; $J_{max,a}^{25}$: $V_{cmax,a}^{25}$, ratio of maximum Rubisco carboxylation velocity over maximum rate of electron transport, both normalized to 25°C; $V_{cmax,N}^{25}$, ratio of maximum carboxylation velocity of Rubisco normalized to 25°C per unit leaf N; n_A, total fraction of leaf N allocated to photosynthetic metabolism; n_P, fraction of leaf N in pigment–protein complexes; n_R, fraction of leaf N in Rubisco; and n_E, fraction of leaf N in electron transport. Values are overall mean ± SD of leaf traits for lowland and upland sites. Significantly different means are indicated by different letters ($P < 0.05$).

Fig. 2 Log-log plots of (a) leaf nitrogen (N) area (N_a) and (b) leaf phosphorus (P) area (P_a) in relation to leaf mass per unit leaf area (M_a). Data points represent individual leaf values (149 lowland species and 97 upland species). Standardized major axis (SMA) tests for common slopes revealed significant differences when comparing $N_a \leftrightarrow M_a$ and $P_a \leftrightarrow M_a$ relationships between lowland and upland species. Closed symbols, lowland species; open symbols, upland species. SMA regressions: solid line, lowland species; dashed line, upland species. SMA regressions are given only when the relationships are significant ($P < 0.05$); refer to Supporting Information Table S3.

electron transport ($J_{max,a}$), using values normalized to a measuring temperature of 25°C (i.e. $V_{cmax,a}^{25}$ and $J_{max,a}^{25}$). Site mean values of $V_{cmax,a}^{25}$ and $J_{max,a}^{25}$ were significantly higher in the upland class ($V_{cmax,a}^{25}$ and $J_{max,a}^{25}$ were 36 and 45% higher, respectively, in the upland class; Table 2; $P < 0.05$), reflecting the parameters' negative relationships with MAT (Fig. S1a,b). Similarly, the mean $V_{cmax,N}$ at 25°C ($V_{cmax,N}^{25}$) of the upland group was greater than that of lowland counterparts (Table 2; $P < 0.05$). Thus, when assessed at a common T and when controlling for elevation differences in C_i (by adopting V_{cmax}), photosynthetic N-use efficiency was, on average, greater at high elevations. Importantly, considerable within-site variability was observed for all three parameters ($V_{cmax,a}^{25}$, $J_{max,a}^{25}$, and $V_{cmax,N}^{25}$) (Fig. 3; Table S1), highlighting the heterogeneity of these key photosynthetic traits among trees within each site. Within-site variability

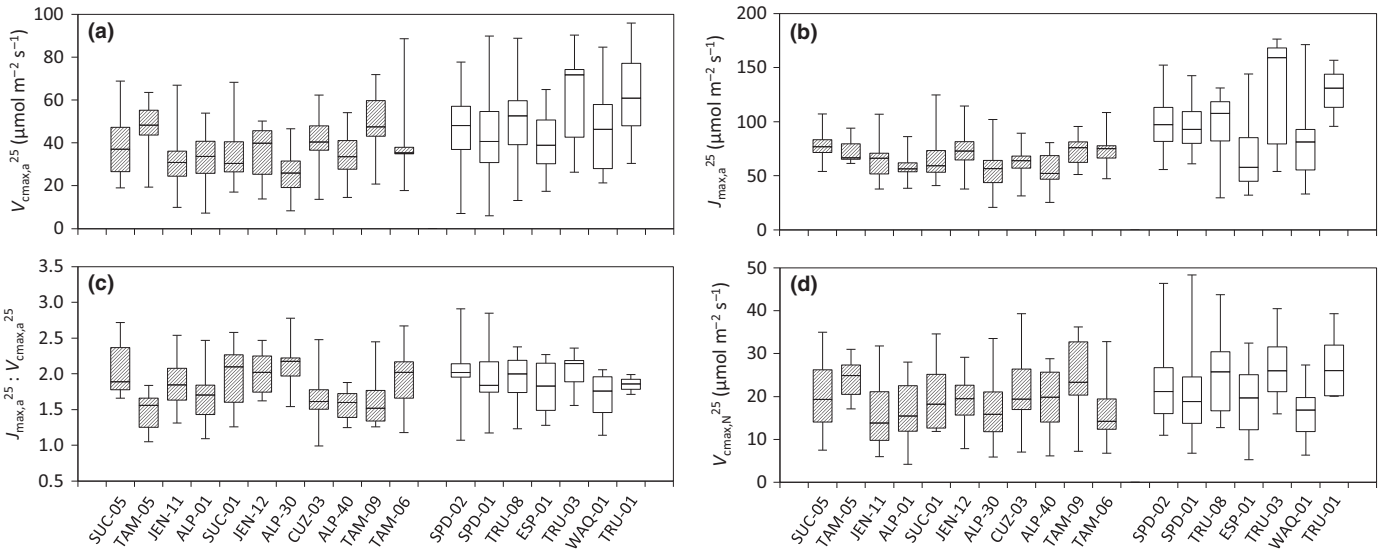

Fig. 3 Box and whisker plots of (a) maximum carboxylation velocity of Rubisco normalized to 25°C ($V_{cmax,a}^{25}$), (b) maximum rate of electron transport normalized to 25°C ($J_{max,a}^{25}$), (c) $J_{max,25}$: $V_{cmax,25}$ ratio, and (d) ratio of $V_{cmax,a}^{25}$ over leaf nitrogen (N) ($V_{cmax,N}^{25}$) for each site. Values are expressed on an area basis. Sites are arranged according to decreasing leaf N : phosphorus (P) for lowland sites and increasing elevation for upland sites. The upper and lower edges of each box indicate the 75th and 25th percentiles, respectively. The horizontal line within each box is the median and the vertical bars indicate the 10th to the 90th percentile ranges.

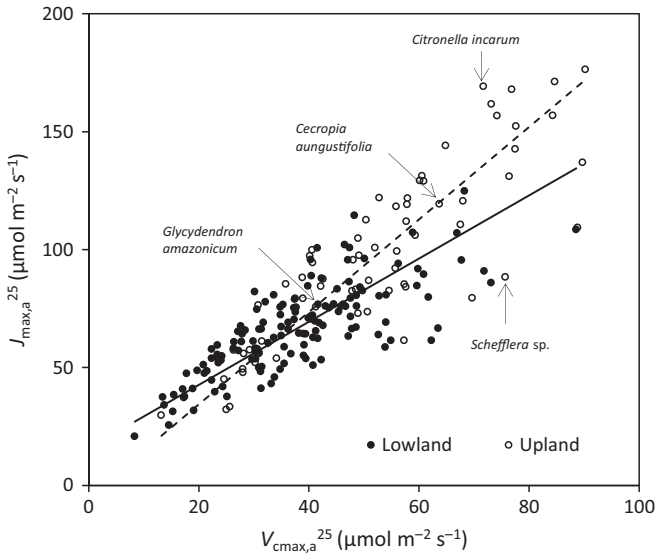

Fig. 4 Plot of maximum carboxylation velocity of Rubisco normalized to 25°C ($V_{cmax,a}^{25}$) against maximum rate of electron transport normalized to 25°C ($J_{max,a}^{25}$). Data points represent individual leaf values (138 lowland species and 69 upland species). Arrows correspond to the four species depicted in the $A \leftrightarrow C_i$ curves in Fig. 1. Closed symbols, lowland species; open symbols, upland species.

was particularly pronounced at the upland sites (Fig. 3; Table S1).

Variations in $J_{max,a}^{25}$ were strongly correlated with $V_{cmax,a}^{25}$, both for lowland ($r^2 = 0.59$) and upland classifications ($r^2 = 0.75$) (Fig. 4). Overall, the $J_{max,a}^{25} \leftrightarrow V_{cmax,a}^{25}$ relationship was similar in the two elevation groups, with mean $J_{max,a}^{25}$: $V_{cmax,a}^{25}$ ratios being statistically equivalent in lowland and upland classes (Table 2). Importantly, marked differences in $J_{max,a}^{25}$: $V_{cmax,a}^{25}$ ratios were observed among individuals (Figs 3, 4), underpinned by fundamental differences in the CO_2 response of net photosynthesis (e.g. Fig. 1b). In most leaves, $J_{max,a}^{25}$ and $V_{cmax,a}^{25}$ co-varied, resulting in relatively constant $J_{max,a}^{25}$: $V_{cmax,25}$ ratios, as illustrated by data from individual plants of *Cecropia angustifolia* and *Glycydendron amazonicum* where the $J_{max,a}^{25}$: $V_{cmax,a}^{25}$ ratio was 1.8 (Figs 1a, 4). However, some leaves exhibited high $V_{cmax,a}^{25}$ but low $J_{max,a}^{25}$ (Fig. 1b; individual of *Schefflera* sp., where $J_{max,a}^{25}$: $V_{cmax,a}^{25}$ = 1.1) while other leaves with a similar $V_{cmax,a}^{25}$ had markedly higher $J_{max,a}^{25}$ (e.g. the *Citronella incarum* individual in Fig. 1b) leading to a higher $J_{max,a}^{25}$: $V_{cmax,a}^{25}$ value (2.4). Such variations in $J_{max,a}^{25}$ and $V_{cmax,a}^{25}$ probably reflect intra- and/or inter-specific variations in relative allocation of N allocation to Rubisco vs electron transport/bioenergetics.

Bivariate relationships

Across all 18 sites, $V_{cmax,a}^{25}$ and $J_{max,a}^{25}$ exhibited positive correlations with soil P, soil N and elevation, and negative correlations with MAT (Table S2); the strength of these relationships was greater for $J_{max,a}^{25}$ than $V_{cmax,a}^{25}$. Relationships with MAP were either weak ($J_{max,a}^{25}$) or not significant ($V_{cmax,a}^{25}$) (Table S2). Across all sites, variations in $V_{cmax,a}^{25}$ and $J_{max,a}^{25}$ were also correlated with leaf chemical composition traits (Table S2), with bivariate relationships being stronger with P_a ($P < 0.01$; $r^2 = 0.11$ for $V_{cmax,a}^{25}$; $r^2 = 0.13$ for $J_{max,a}^{25}$) than N_a ($P < 0.01$; $r^2 = 0.05$ for both $V_{cmax,a}^{25}$ and $J_{max,a}^{25}$). Leaf N : P ratios exhibited weak, negative correlations with $V_{cmax,a}^{25}$ and $J_{max,a}^{25}$ ($P < 0.01$; $r^2 = 0.08$ for $V_{cmax,a}^{25}$, $r^2 = 0.06$ for $J_{max,a}^{25}$; Table S2). No significant relationship was found between $V_{cmax,a}^{25}$ and M_a, whereas the $J_{max,a}^{25} \leftrightarrow M_a$ relationship was significant ($P < 0.05$; $r^2 = 0.04$; Table S2).

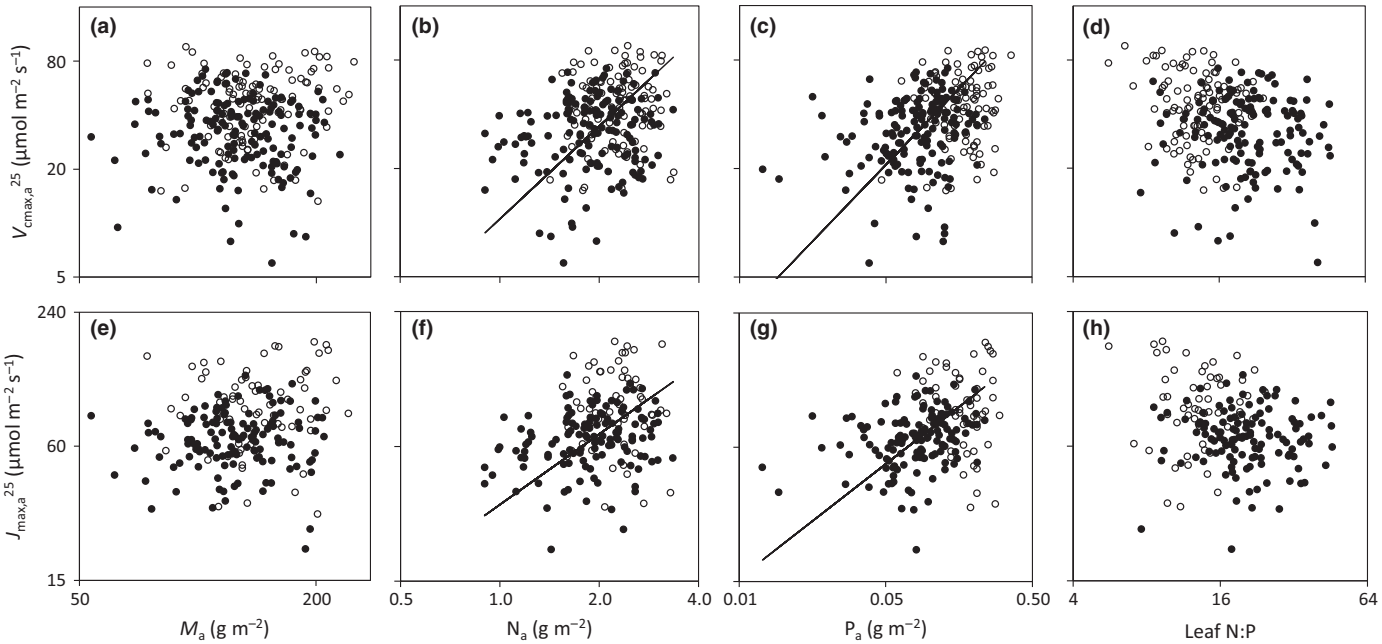

Fig. 5 Upper panels: log-log plots of maximum carboxylation velocity of Rubisco normalized to 25°C ($V_{cmax,a}^{25}$) in relation to (a) leaf mass per unit leaf area (M_a), (b) leaf nitrogen (N) area (N_a), (c) leaf phosphorus (P) area (P_a) and (d) leaf N : P. Data points represent individual leaf values (150 lowland species and 95 upland species). Standardized major axis (SMA) tests for common slopes revealed significant differences when comparing $V_{cmax,a}^{25} \leftrightarrow N_a$, $V_{cmax,a}^{25} \leftrightarrow P_a$ and $V_{cmax,a}^{25} \leftrightarrow$ leaf N : P relationships between lowland and upland species, but no significant difference when comparing slopes of $V_{cmax,a}^{25} \leftrightarrow M_a$ relationships between lowland and upland species. Lower panels: log-log plots of maximum rate of electron transport normalised to 25°C ($J_{max,a}^{25}$) in relation to (e) M_a, (f) N_a, (g) P_a and (h) leaf N : P. Data points represent individual leaf values (127 lowland species and 58 upland species). SMA tests for common slopes revealed significant difference when comparing $J_{max,a}^{25}$ and leaf traits relationships between lowland and upland species. Closed symbols, lowland species; open symbols, upland species. SMA regressions are given only when the relationships are significant ($P < 0.05$); refer to Supporting Information Table S3.

When assessed among upland sites, no significant relationships were found between $V_{cmax,a}^{25}$, M_a, N_a, P_a or N : P ratio (Fig. 5a–d). For lowland sites, $V_{cmax,a}^{25}$ was positively related to P_a ($P = 0.013$; $r^2 = 0.04$; Table S3) and N_a ($P = 0.050$; $r^2 = 0.02$; Table S3), but not leaf N : P ratio or M_a (Fig 5a–d). The absence of an N : P effect for upland or lowland classes was consistent with SMA analyses comparing the slopes of $V_{cmax,a}^{25} \leftrightarrow N_a$, $V_{cmax,a}^{25} \leftrightarrow P_a$ and $V_{cmax,a}^{25} \leftrightarrow M_a$ for the lowland class, split according to leaf N : P ratios below and above 20 – this ratio generally being thought indicative of the N : P ratio above which physiological processes are more likely to be limited by P as opposed to N (and vice versa) (Güsewell, 2004). No significant difference in the slopes of the relationships was found ($P > 0.05$; data not shown). Similar patterns were observed for $J_{max,a}^{25}$ (Fig. 5e–h), which was positively related to N_a ($P = 0.012$; $r^2 = 0.05$; Table S3) and P_a ($P = 0.002$; $r^2 = 0.08$; Table S3) for the lowland class only.

Investigating whether variations in photosynthetic N-use efficiency were related to M_a, both across all sites (Table S2) and within each elevation class (Fig. 6a), there was no significant $V_{cmax,N}^{25} \leftrightarrow M_a$ relationship across all 18 sites (Table S2) or within the upland elevation class (Table S3). Nevertheless, for

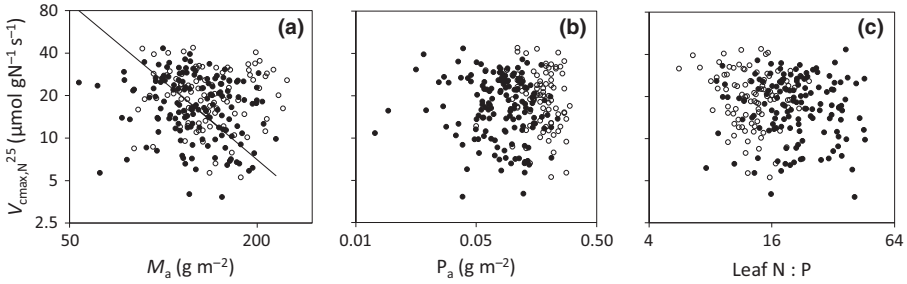

Fig. 6 Log–log plots of the ratio of maximum carboxylation velocity of Rubisco normalized to 25°C ($V_{cmax,a}^{25}$) to leaf nitrogen (N) ($V_{cmax,N}^{25}$) in relation to (a) leaf mass per unit leaf area (M_a), (b) leaf phosphorus (P) area (P_a) and (c) leaf N : P. Data points represent individual leaf values (150 lowland species and 95 upland species). Standardized major axis (SMA) tests for common slopes revealed a significant difference only when comparing $V_{cmax,N}^{25} \leftrightarrow P_a$ between lowland and upland species. Symbols: closed symbols, lowland species; open symbols, upland species. SMA regressions are given only when the relationships are significant ($P < 0.05$); refer to Supporting Information Table S3.

the lowland class, a weak negative $V_{cmax,N}^{25} \leftrightarrow M_a$ relationship was observed ($P = 0.01$; Table S3). On average, $V_{cmax,N}^{25}$ at a given M_a was higher in upland species than in their lowland counterparts. With respect to foliar P, there was no significant relationship between $V_{cmax,N}^{25}$ and leaf P_a or leaf N : P ratio when considering the elevation classes separately. This conclusion held for $V_{cmax,N}^{25} \leftrightarrow P_a$ when combining upland and lowland data (Table S2). For $V_{cmax,N}^{25} \leftrightarrow$ N : P, combining upland and lowland data resulted in a weak significant relationship ($P < 0.05$; $r^2 = 0.02$; Table S2); similarly, relationships between $V_{cmax,N}^{25}$ and soil P, soil N and elevation were relatively weak (Table S2). Collectively, these results show that the proportion of the variance in $V_{cmax,N}^{25}$ accounted for by the above soil- and leaf-level parameters was negligible.

Variation in N-allocation patterns

To further explore what factors might contribute to variations in $V_{cmax,N}^{25}$, we calculated the fraction of leaf N allocated to photosynthesis (n_A); n_A is dependent on the allocation of leaf N to Rubisco (n_R), electron transport (n_E) and pigment–protein complexes (n_P). Fig. 7 shows that mean values of n_A and its underlying components exhibited relatively little variation across sites. Nevertheless, inter-specific variations were evident at each site, with n_R varying up to seven-fold at some sites (e.g. CUZ-03; 0.03–0.20; Table S1). A large proportion of N was inferred to be allocated to pigment–protein complexes, with n_P being greater than n_R and n_E combined. The overall mean of n_R for the upland class (0.105) was significantly higher than that for the lowland class (0.090; Table 2; $P < 0.05$). Similarly, n_E was higher for upland (0.034) than for lowland groups (0.028; Table 2; $P < 0.05$). There was no difference between the elevation classes in n_P. Overall, n_A was similar in the lowland and upland groupings (37–38%; Table 2).

There was considerable variability in n_A among lowland and upland species (0.1–0.6), with significant negative correlations being found with M_a, N_a and P_a for the lowland group (Fig. 8; Table S5). Similar significant correlations existed for the upland class but with the important caveat that upland species consistently exhibited higher n_A at a given N_a and P_a (Figs 8, S2; Table S5). Thus, while mean values of n_A were similar in upland and lowland species, the fraction of leaf N allocated to photosynthesis was greater in upland plants when comparisons were made at common leaf N_a and P_a values.

Validation of Rubisco estimates by *in vitro* assays

We used *in vitro* Rubisco assays on 16 lowland species (Fig. 9a) to quantify n_R, thus allowing direct comparison with that of the *in vivo* estimates derived from $V_{cmax,a}^{25}$. Fig. 9(b) shows that there was considerable discrepancy between *in vitro* and *in vivo* predicted n_R. If one assumes that the *in vitro* values provide an estimate of potential Rubisco capacity, and that the *in vivo* values are indicative of the realized maximum rate in intact tissues, then it is possible that the *in vivo* approach underestimates the proportion of N allocated in Rubisco. Reliance on the *in vitro* values resulted in marked increases in n_R at a given M_a, albeit the overall pattern of increasing n_R with decreasing M_a still held (Fig. S3a). Considering the overall N investment pattern in photosynthetic metabolism, adopting *in vitro* estimates of n_R resulted in marked increases in the total fraction of N allocated to photosynthesis compared with *in vivo* estimates (Fig. S4). Indeed, in some cases *in vitro* estimates of N allocation to Rubisco was similar to, or even higher than, N allocation to pigment−protein complexes (Fig. S4). Collectively, these results suggest that the answer to the question '*How much leaf N is allocated to photosynthesis*' will depend on whether *in vivo* or *in vitro* estimates of n_R are used in the underlying calculations.

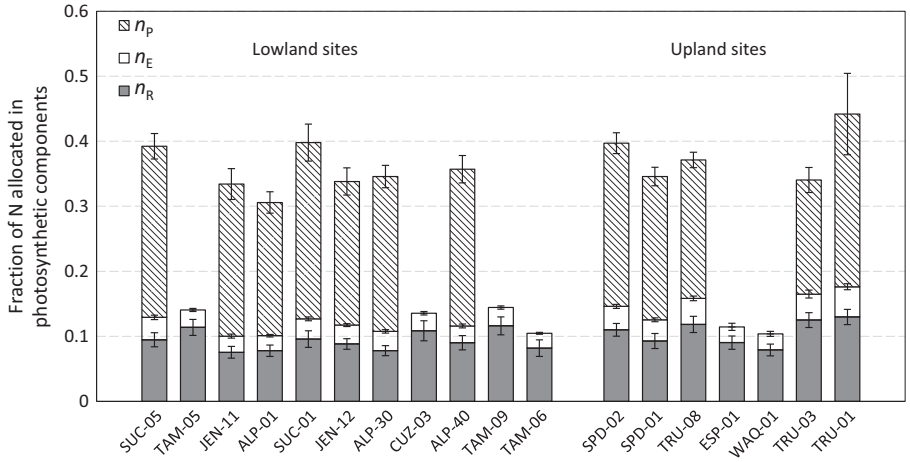

Fig. 7 Stacked graph showing the fraction of leaf nitrogen (N) in pigment–protein complexes (n_P), in electron transport (n_E), and the in Rubisco (n_R) for each site. n_R was estimated from the maximum carboxylation velocity of Rubisco (normalized to 25°C), $V_{cmax,a}^{25}$; n_E was estimated from the maximum electron transport rate (normalized to 25°C), $J_{max,a}^{25}$; and n_P was estimated from the chlorophyll concentration. n_P values were unavailable for six sites as a consequence of thawing of leaf samples. Sites are arranged according to decreasing leaf N : P for lowland sites and increasing elevation for upland sites. Error bars, ± SE of mean.

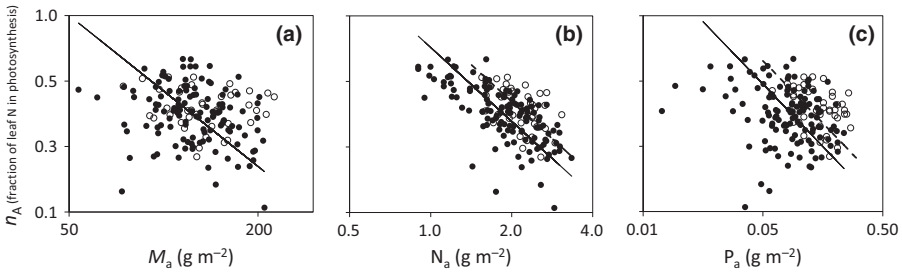

Fig. 8 Log-log plots of the total fraction of leaf nitrogen (N) allocated to photosynthetic metabolism (n_A) in relation to (a) leaf mass per unit leaf area (M_a), (b) leaf N area (N_a) and (c) leaf phosphorus (P) area (P_a). Data points represent individual leaf values (126 lowland species and 40 upland species). Standardized major axis (SMA) tests for common slopes revealed no significant difference when comparing relationships between lowland and upland species, but with the elevation (i.e. *y*-axis intercept) of the bivariate relationship being higher in upland species than in lowland species. Closed symbols, lowland species; open symbols, upland species. SMA regressions: solid line, lowland species; dashed line, upland species. SMA regressions are given only when the relationships are significant ($P < 0.05$); refer to Supporting Information Table S5.

Modelling variations in $V_{cmax,a}^{25}$, $J_{max,a}^{25}$ and $V_{cmax,N}^{25}$

We used linear mixed-effects to model variations in $V_{cmax,a}^{25}$, $J_{max,a}^{25}$ and $V_{cmax,N}^{25}$; the starting model included only continuous explanatory terms for leaf traits and environmental variables. Additional details of the model selection procedure are provided in Table S6. When presented with information on soil and leaf P and N as key nutrients driving maximum carboxylation capacity of Rubisco, the final preferred model for $V_{cmax,a}^{25}$ (model 6; Table S6) retained P only, suggesting an increase of $V_{cmax,a}^{25}$ as soil and foliar P increase (Table 3). A combination of site-level soil P and individual-level foliar P as fixed effects, and family as a random effect, explained 39% of the variation in $V_{cmax,a}^{25}$ (Fig. S5). Inclusion of MAT, soil N, leaf N_a, M_a and effective cation exchange capacity of soils as fixed effects did not improve model performance (Table S6). The model's variance components, as defined by the random term, indicated that family accounted for only 2.5% of the unexplained variance (i.e. the response variance not accounted for by the fixed terms) (Table 3). Finer phylogenetic detail (genera and species) did not improve the model. A review of diagnostic plots from the final preferred model showed that inclusion of elevation class did not improve model performance given the prior inclusion of environmental variables that describe the elevation gradient (e.g. soil P, soil N and MAT).

Similar to $V_{cmax,a}^{25}$, variations in $J_{max,a}^{25}$ were largely accounted for by a combination of site-level soil P and individual-level foliar P, with $J_{max,a}^{25}$ increasing with increasing soil and foliar P (Table 3); the final model explained 44% of the variation in $J_{max,a}^{25}$ (Fig. S5). The preferred model (determined by assessing the effect of dropping sequentially explanatory variables; Table S6) did not retain soil N, leaf N_a, M_a or MAT (Table S6). For the random effects, family contributed 2.8% to the unexplained variance (Table 3).

For $V_{cmax,N}^{25}$ (i.e. photosynthetic N-use efficiency), we attempted to construct a model using combinations of soil and leaf P, soil and leaf N, soil ECEC, and climate (MAT). However, in contrast to $V_{cmax,a}^{25}$ and $J_{max,a}^{25}$, no combination of available explanatory variables produced a model superior to a null construct that merely allowed for variation around the data-set mean value of $V_{cmax,N}^{25}$. This suggests that other factors, such as how leaf N is allocated and/or whether Rubisco is fully active, may have played a role.

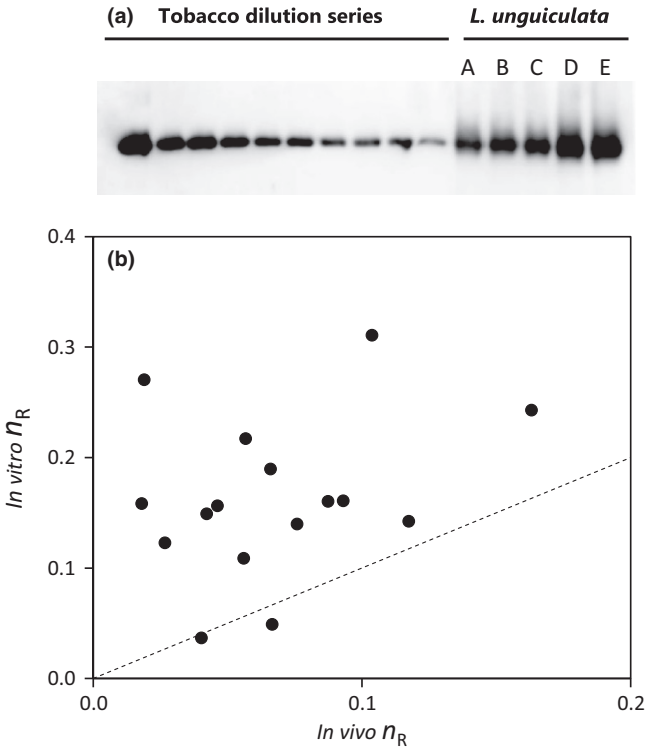

Fig. 9 (a) SDS-PAGE profile of Rubisco extracted from frozen fresh leaf discs. Individual bands show large subunits of Rubisco. The last five bands on the right side (A–E) correspond to 0.47, 0.54, 0.57, 0.78 and 1.21 g m^{-2} of Rubisco for lowland species (*Licania unguiculata* from the Chrysobalanaceae family), which then translate to values for the fraction of leaf N in Rubisco (n_R) of 0.03, 0.04, 0.04, 0.06 and 0.09. In this case, the final value of *in vitro* n_R for *L. unguiculata* was 0.04, as calculated from A–C, as these values fall within the tobacco standard curve. The standard curve was obtained for a dilution series of tobacco Rubisco. (b) *In vitro* n_R estimated from a Rubisco western blot assay plotted against *in vivo* n_R derived from the maximum carboxylation velocity of Rubisco (normalized to 25°C), $V_{cmax,a}^{25}$. $n = 16$. The dashed line indicates the 1 : 1 relationship.

Table 3 Output from linear mixed-effects models, with $V_{cmax,a}^{25}$ (maximal capacity of carboxylation by Rubisco per unit leaf area, at 25°C) and $J_{max,a}^{25}$ (maximal capacity of photosynthetic electron transport per unit leaf area, at 25°C) as the response variables, each showing fixed and random effects

Final model ($V_{cmax,a}^{25}$)			
Fixed effect	Estimate	SE	*t* value
Intercept	41.470	1.578	26.288
Log_{10} (soil P)	7.909	2.466	3.207
P_a	68.148	22.558	3.021
Random effect		Variance	% of total
Intercept variance: family		45.568	2.49%
Residual error (within family)		1783.626	97.51%
			100.00%
AIC	1645.6		
BIC	1662.0		
-2LL	−817.8		

Final model ($J_{max,a}^{25}$)			
Fixed effect	Estimate	SE	*t* value
Intercept	77.217	2.712	28.477
Log_{10} (soil P)	16.866	4.327	3.898
P_a	94.483	40.245	2.348
Random effect		Variance	% of total
Intercept variance: family		121.3	2.79%
Residual error (within family)		4232.9	97.21%
			100.00%
AIC	1342.4		
BIC	1357.3		
-2LL	−666.2		

$V_{cmax,a}^{25} = 41.47 + (7.91 \times \log_{10}[\text{soil P}]) + (68.15 \times P_a)$
$J_{max,a}^{25} = 77.22 + (16.87 \times \log_{10}[\text{soil P}]) + (94.48 \times P_a)$

Predictive equations for $V_{cmax,a}^{25}$ and $J_{max,a}^{25}$ based on final preferred models are shown at the bottom. For the $V_{cmax,a}^{25}$ and $J_{max,a}^{25}$ model, the fixed component explanatory variables were soil P and leaf P. Parameter estimate, standard error (SE) and *t*-values are given for the explanatory variables. The best predictive models were selected based on a stepwise selection process outlined in Supporting Information Table S6. Before inclusion in the models, continuous explanatory variables were centred on the population mean. For equations that are not centred on the population mean (i.e. using absolute values), the *y*-axis intercept values are altered, yielding non-centred equations as follows: $V_{cmax,a}^{25} = 12.82 + (7.91 \times \log_{10}[\text{soil P}]) + (68.15 \times \text{Pa})$; $J_{max,a}^{25} = 24.07 + (16.87 \times \log_{10}[\text{soil P}]) + (94.48 \times \text{Pa})$.

Discussion

Regional and inter-biome context

Past studies on forest biomes revealed variability in the slope of $V_{cmax,a}^{25} \leftrightarrow N_a$ relationships, with lower rates of V_{cmax} per unit N in nutrient-poor, lowland tropical forests compared with lowland forests on more fertile soils, upland tropical forests and temperate broadleaf forests (Carswell *et al.*, 2000; Domingues *et al.*, 2007, 2010; Meir *et al.*, 2007; Kattge *et al.*, 2009; Mercado *et al.*, 2011; van de Weg *et al.*, 2012). Moreover, Reich *et al.* (2009) concluded that the slope of mass-based $A \leftrightarrow N$ relationships is lower in the tropics than in colder arctic and temperate biomes. Our study supports such studies, with $V_{cmax,N}^{25}$ values for our upland and lowland TMFs (22.5 and 18.9 μmol CO_2 g N^{-1} s^{-1}, respectively) being markedly lower than those reported for temperate broadleaved trees (34 μmol CO_2 g N^{-1} s^{-1}; Kattge *et al.*, 2009).

How do our results compare with other analyses of photosynthetic capacity in tropical ecosystems? The ranges of $V_{cmax,a}^{25}$ (6–96 μmol m^{-2} s^{-1}; Table S1) and $J_{max,a}^{25}$ (21–176 μmol m^{-2} s^{-1}; Table S1) values from our study were wider than those reported for drier tropical sites in West Africa (Domingues *et al.*, 2010), perhaps reflecting environmental differences, or differences in the number of species sampled (210 here vs 39 in the West African study). For our lowland TMFs (which included three low nutrient status white sand sites in northern Peru), the overall mean $V_{cmax,a}^{25}$ (36 ± 15 μmol m^{-2} s^{-1}) was lower than previously reported tropical values: Carswell *et al.* (2000): 43 μmol m^{-2} s^{-1}; Domingues *et al.* (2007): 53 μmol m^{-2} s^{-1}; Meir *et al.* (2007): 49–68 μmol m^{-2} s^{-1}; Kattge *et al.* (2009): 41 μmol m^{-2} s^{-1} (nonoxisol); Bloomfield *et al.* (2014a): 63 μmol m^{-2} s^{-1}; Domingues *et al.* (2015): 39–46 μmol m^{-2} s^{-1}. By contrast, our mean $V_{cmax,a}^{25}$ values were higher than the values for lowland TMFs only growing on nutrient-poor oxisol (29 μmol m^{-2} s^{-1}; Kattge *et al.*, 2009). As $J_{max,a}^{25}$ was tightly correlated with $V_{cmax,a}^{25}$ (Fig. 4), our estimates of $J_{max,a}^{25}$ for lowland TMFs were also lower than those reported in the above-mentioned studies. Rates of $V_{cmax,a}^{25}$ at our upland sites (49 ± 20 μmol m^{-2} s^{-1}) were similar to those reported by van de Weg *et al.* (2012): 56 μmol m^{-2} s^{-1} for the same Andean region, and fell in the middle of the range of values reported in Dusenge *et al.* (2015) and Vårhammar *et al.* (2015) for high-elevation tropical trees of Rwanda.

Taken together, our results support the hypothesis that both $V_{cmax,a}^{25}$ and photosynthetic N efficiency are lower in lowland TMFs than in temperate broadleaved forests. In addition, each parameter is highly variable, both among co-existing tropical species growing at individual sites and between environmentally contrasting sites.

Phosphorus – does it modulate photosynthetic capacity and/or N-use efficiency?

Our site selection aimed to assess the potential effect of P limitation on photosynthetic performance across TMFs in western Amazonia and the Andes where substantial variations in soil P occur (lowland sites: 38–727 mg P kg^{-1}; upland sites: 496–1631 mg P kg^{-1}). Low P availability can limit rates of photosynthesis via reduced maximal rates of RuBP regeneration (i.e. J_{max}), with maximal Rubisco activity (i.e. V_{cmax}) also often being reduced (Brooks, 1986; Jacob & Lawlor, 1992; Loustau

et al., 1999). While the mechanisms responsible for reduced V_{cmax} remain uncertain, possible factors include the need to maintain co-limitation by RuBP regeneration and carboxylation, as well as feedback inhibition on Rubisco resulting from the inability to export triose phosphates to the cytosol (Wullschleger, 1993; Walker *et al.*, 2014).

The hypothesis that photosynthetic capacity would be positively correlated with soil [P] and leaf P_a was supported by our results – a finding consistent with earlier studies on tropical species in South America, West Africa and Australia (Domingues *et al.*, 2007, 2010; Meir *et al.*, 2007; Kattge *et al.*, 2009; Bloomfield *et al.*, 2014b). Among lowland sites alone, and the combination of lowland and upland sites together, significant positive relationships were observed between photosynthetic capacity (expressed as either $V_{cmax,a}{}^{25}$ or $J_{max,a}{}^{25}$) and foliar P_a, and soil [P] (Tables S2, S3). Across all 18 TMF sites, $V_{cmax,a}{}^{25}$ and $J_{max,a}{}^{25}$ also exhibited significant negative relationships with leaf N : P (Table S2). Moreover, foliar P_a and soil [P] emerged as significant explanatory variables in linear mixed-effect models of variations in photosynthetic capacity (Table 3), accounting for ~40% of the observed variations in $V_{cmax,a}{}^{25}$ and $J_{max,a}{}^{25}$. That MAT was not retained in the preferred models suggests that, while growth temperature can affect photosynthetic capacity (Hikosaka *et al.*, 2006; Sage & Kubien, 2007) and patterns of N investment, knowledge of growth temperature along the western Amazon–Andes elevation gradient is not required when data on leaf and soil P are available.

Past studies reported that P deficiencies also reduce photosynthetic N-use efficiency (Reich *et al.*, 2009) and the fraction of leaf N allocated to photosynthesis (Warren & Adams, 2002). While average values $V_{cmax,N}$ and foliar [P] were highest in our upland trees, no significant $V_{cmax,N} \leftrightarrow P_a$ relationships were observed, either across all sites or within each elevation class. Furthermore, we could not identify key factors explaining variation in $V_{cmax,N}$ using linear mixed-effects models; this included models that contained data on soil and foliar [P]. While this does not preclude a role for deficiencies in cytosolic [P] in regulating *in vivo* values of $V_{cmax,N}$, it seems unlikely that either soil or total leaf [P] can be used as a predictor of variations in *in vivo* Rubisco capacity per unit leaf N.

Activation state of Rubisco

In vitro quantification in several lowland TMF species revealed that Rubisco content inferred from CO_2 response curves may have substantially underestimated absolute contents of this key protein (Fig. 9). When estimating Rubisco abundance from $A \leftrightarrow C_i$ curves, Rubisco is assumed to be fully activated – however, there is growing evidence that Rubisco often operates at less than maximum activity or is in excess of CO_2 fixation requirements (Stitt & Schulze, 1994; Warren *et al.*, 2000). Partial activation could be linked to limitations in sink demand for carbohydrates and/or co-limitation by other rock-derived nutrients such as calcium (e.g. Asner *et al.*, 2014b). Inactive Rubisco might serve as a temporary N store – as such, Rubisco can act as both a metabolic and nonmetabolic protein (Stitt & Schulze, 1994; Warren *et al.*, 2000). Viewed from this perspective, *in vivo* estimates of V_{cmax} provide insights into N investment in the *metabolically active* Rubisco, relevant when modelling gross primary productivity of TMF ecosystems. However, if the objective is to assess how plants differ in N investment in both active and inactive forms of Rubisco, then n_R estimated using other approaches, such as western blots (or similar quantitative techniques), might be required.

As noted earlier in the Discussion, the observed values of $V_{cmax,N}{}^{25}$ were lower than that of trees growing in temperate environments (Kattge *et al.*, 2009). Similarly, when compared at any given M_a, *in vivo* estimates of n_R (i.e. the fraction of leaf N allocated to Rubisco estimated from gas exchange) were, on average, lower in our TMF trees compared with the global average (Hikosaka, 2004; Wright *et al.*, 2004) (Fig. S3). By contrast, *in vitro* estimates of n_R (i.e. n_R estimated from protein extraction) were often higher than the global average (Fig. S3). This finding raises the possibility that the efficiency of N investment in Rubisco may not necessarily be lower in TMFs; rather, it may be that the activation state is lower in tropical forests compared with their temperate counterparts. Further work is needed to explore this question; additional work is also needed to determine what effect, if any, limitations in mesophyll conductance (g_m) have on estimates of V_{cmax} and the associated values of n_R.

Additional factors influencing V_{cmax} estimates

In our study, we have so far estimated *in vivo* rates of $V_{cmax,a}{}^{25}$ assuming a common, single set of kinetic constants (K_c and K_o) for Rubisco (von Caemmerer *et al.*, 1994) and associated activation energies (E_a) (Farquhar *et al.*, 1980), as well as infinite g_m. Such assumptions were made necessary in the absence of K_c, K_o, E_a and g_m values for tropical species. Application of different K_c and K_o values, such as those reported by Bernacchi *et al.* (2002), would alter estimates of $V_{cmax,a}{}^{25}$ for all trees but would not alter relative differences among sites or elevational classes. By contrast, application of Bernacchi *et al.* (2002) E_a values for K_c and K_o (80.99 and 23.72 kJ mol^{-1}, respectively), and V_{cmax} (65.3 kJ mol^{-1}) could potentially produce relative differences in $V_{cmax,a}{}^{25}$ between upland and lowland trees, depending on the extent to which leaf temperatures differed among the sites. Similarly, replacement of the Farquhar *et al.* (1980) E_a values of V_{cmax} and J_{max} (of 64.8 and 37.0 kJ mol^{-1}, respectively) with those of Bernacchi *et al.* (2002) (65.3 and 43.9 kJ mol^{-1}, respectively) could alter the relative differences in $V_{cmax,a}{}^{25}$ and $J_{max,a}{}^{25}$ between upland and lowland sites. To check whether application of alternative E_a values changed our conclusions regarding site-to-site differences, we calculated $V_{cmax,a}{}^{25}$ and $J_{max,a}{}^{25}$ using the respective activation energies of Farquhar *et al.* (1980) and Bernacchi *et al.* (2002). Use of the Bernacchi *et al.* (2002) E_a values resulted in an average 10.6% increase in estimates of V_{cmax25} for lowland trees (Table S7), reflecting the fact that lowland leaf temperatures were near 30°C (Table S4). Upland estimates were less affected (3.5% increase; Table S7) as the average leaf temperature of upland group was 25.7°C (Table S4). Despite the increased estimates of V_{cmax25} for lowland trees when using E_a values from Bernacchi *et al.* (2002), there remained a significant difference between lowland and upland mean V_{cmax25} values (Table S7); the

same was true for $J_{max,a}^{25}$ (Table S7). As a result, relationships between photosynthetic properties and site MAT and soil P were similar when using Farquhar *et al.* (1980) and Bernacchi *et al.* (2002) E_a values (Fig. S1). Thus, irrespective of which E_a values are used (see Medlyn *et al.* (2002) for further discussion on the temperature dependence of these constants), we are confident that mean values of V_{cmax25} and $J_{max,a}^{25}$ are indeed higher in the upland plants growing in the Peruvian Andes.

What impact might systematic differences in g_m between upland and lowland TMFs have on our results? If g_m was finite, but similar in upland and lowland TMF environments, then our conclusion that $V_{cmax,a}^{25}$ is higher in upland species would hold (albeit with modified values). However, if g_m was more limiting in lowland TMF trees than in their upland counterparts, then calculation of V_{cmax} using $A-C_c$ curves might fail to differentiate between the upland and lowland groups. A definitive assessment of this issue will require further work assessing g_m in tropical trees (e.g. using concurrent measurements of leaf gas exchange and carbon isotope discrimination or chlorophyll fluorescence). Although g_m tends to decrease with increasing M_a (Flexas *et al.*, 2008), the M_a difference between lowland and upland groups was small (Table 1). Given the potential for large variations in g_m among species (at a given M_a), it is unlikely that g_m would have been higher in the selected lowland TMF trees. Irrespective of the effect of elevation on g_m, rates of $A_{40,a}$ and $A_{200,a}$ (measured at prevailing leaf Ts) were surprisingly high in plants at the cooler, high-elevation sites (Table S4). Given this and our extensive sample size, we feel confident that photosynthetic capacity at a standardized T is probably larger in trees growing at high elevations in the Andes compared with those in the lowland regions of Amazonia, as proposed by van de Weg *et al.* (2012, 2014). Enhanced photosynthetic capacity at high altitude could help negate the inhibitory effects of low T on leaf-level CO_2 uptake, with the result that gross primary productivity (GPP) would not decline with increasing elevation as much as expected.

Recent modelling of C-exchange processes at a high-elevation TMF site (3025 m asl) in Peru suggested that GPP may be 20–40% lower compared with lowland TMFs (Girardin *et al.*, 2014a; van de Weg *et al.*, 2014); low T appeared to be most important factor limiting GPP at high elevations (van de Weg *et al.*, 2014). Our results suggest that the inhibitory effect of low T on GPP of upland TMFs would be greater if photosynthetic capacity remained constant across the elevation gradient. Thus, the greater photosynthetic capacity of upland TMFs might contribute to GPP being relatively homeostatic across the Peruvian Amazon–Andes elevation gradient. Further work is needed to explore how elevation-dependent variations in photosynthetic capacity impact on current and future net primary productivity (NPP) of TMFs, when taking into account other NPP components (e.g. leaf area index, biomass allocation, litter fall and autotrophic respiration).

Concluding statements

Our findings reveal greater photosynthetic capacity in Andean forest leaves compared with lowland western Amazonian leaves, underpinned by greater concentrations of leaf N and N-use efficiency per unit leaf area (Table 2; Fig. 8). Our data also support the hypothesis that variations in leaf and soil P play a key role in modulating the photosynthetic capacity of TMFs (Fig. 5; Tables 3, S2), with the mixed-effects models (Table 3) providing the modelling community with predictive equations that will enable model parameterization based on arguably the largest single tropical V_{cmax} data set available. Finally, our analyses indicate that a substantial fraction of Rubisco is inactive in trees growing in the Peruvian Amazon and suggest that a greater fraction of leaf N may well be invested in photosynthetic machinery than indicated by leaf gas exchange measurements.

Acknowledgements

We thank R. Tupayachi, N. Jaramillo, F. Sinca, L. Carranza-Jimenez and the Spectranomics team for field and laboratory assistance. Measurements were made in plots inventoried and maintained by RAINFOR (http://www.rainfor.org) investigators from Peru. Access to the field sites was also facilitated by Gordon and Betty Moore Foundation grants (to O.L.P., Y.M., J.L. and G.P.A.). Foliar sampling, taxonomic determinations, and chemical analyses were supported by a grant from the Gordon and Betty Moore Foundation to the Carnegie Institution for Science. This work was also funded by grants/fellowships from the Australian Research Council (DP0986823, DP130101252, CE140100008 and FT0991448 to O.K.A.; and FT110100457 to P.M.), and NERC grants (NE/C51621X/1 and NE/F002149/1 to P.M.). R.G. was supported by a Newton International Fellowship (funded by the Royal Society, the British Academy and the Royal Academy of Engineering). N.H.A.B. is funded by a Malaysian Government Postgraduate Scholarship.

Author contributions

O.K.A., J.L., P.M., Y.M., O.L.P., G.P.A., R.E.M., F.Y.I., L.K.W., R.G., O.S.O., N.H.A.B., J.R.E. and B.M.L. planned and designed the research. N.H.A.B., F.Y.I., L.K.W., R.G., O.S.O., K.J.B., G.P.A., R.E.M., J.L., Y.M., N.S., E.G.C., T.D., C.A.Q., F.S., A.E.V., P.P.Z.C., J.d.A-P., K.Q.H., I.C.T., R.B.L., Y.P.T., J.H.O. and O.K.A. conducted fieldwork and/or analysed field-based data. N.H.A.B., F.Y.I., G.P.A., R.E.M., B.M.L. and J.R.E. performed laboratory experiments and analysed chemical/biochemical data. N.H.A.B., O.K.A., K.J.B., J.L., O.L.P., P.M., G.P.A., Y.M., O.S.O., R.G., L.K.W., J.R.E. and B.M.L. wrote the manuscript.

References

Aerts R, Chapin FSI. 2000. The mineral nutrition of wild plants revisited: a re-evaluation of processes and patterns. *Advances in Ecological Research* **30**: 1–67.

Almeida JP, Montúfar R, Anthelme F. 2012. Patterns and origin of intraspecific functional variability in a tropical alpine species along an altitudinal gradient. *Plant Ecology & Diversity* **6**: 423–433.

Asner GP, Anderson CB, Martin RE, Knapp DE, Tupayachi R, Sinca F, Malhi Y. 2014a. Landscape-scale changes in forest structure and functional traits along an Andes-to-Amazon elevation gradient. *Biogeosciences* **11**: 843–856.

Asner GP, Martin RE. 2011. Canopy phylogenetic, chemical and spectral assembly in a lowland Amazonian forest. *New Phytologist* **189**: 999–1012.

Asner GP, Martin RE, Tupayachi R, Anderson CB, Sinca F, Carranza-Jiménez L, Martinez P. 2014b. Amazonian functional diversity from forest canopy chemical assembly. *Proceedings of the National Academy of Sciences, USA* **111**: 5604–5609.

Ayub G, Smith RA, Tissue DT, Atkin OK. 2011. Impacts of drought on leaf respiration in darkness and light in *Eucalyptus saligna* exposed to industrial-age atmospheric CO_2 and growth temperature. *New Phytologist* **190**: 1003–1018.

Beer C, Reichstein M, Tomelleri E, Ciais P, Jung M, Carvalhais N, Rödenbeck C, Arain MA, Baldocchi D, Bonan GB *et al.* 2010. Terrestrial gross carbon dioxide uptake: global distribution and covariation with climate. *Science* **329**: 834–838.

Bernacchi CJ, Portis AR, Nakano H, von Caemmerer S, Long SP. 2002. Temperature response of mesophyll conductance. Implications for the determination of Rubisco enzyme kinetics and for limitations to photosynthesis *in vivo*. *Plant Physiology* **130**: 1992–1998.

Bloomfield KJ, Domingues TF, Saiz G, Bird MI, Crayn DM, Ford A, Metcalfe D, Farquhar GD, Lloyd J. 2014a. Contrasting photosynthetic characteristics of forest vs. savanna species (far North Queensland, Australia). *Biogeosciences* **11**: 7331–7347.

Bloomfield KJ, Farquhar GD, Lloyd J. 2014b. Photosynthesis–nitrogen relationships in tropical forest tree species as affected by soil phosphorus availability: a controlled environment study. *Functional Plant Biology* **41**: 820–832.

Brooks A. 1986. Effects of phosphorus nutrition on ribulose-1,5-bisphosphate carboxylase activation, photosynthetic quantum yield and amounts of some Calvin-cycle metabolites in spinach leaves. *Australian Journal of Plant Physiology* **13**: 221–237.

Bruhn D, Mikkelsen TN, Atkin OK. 2002. Does the direct effect of atmospheric CO_2 concentration on leaf respiration vary with temperature? Responses in two species of Plantago that differ in relative growth rate. *Physiologia Plantarum* **114**: 57–64.

Bruijnzeel LA, Scatena FN, Hamilton LS. 2011. *Tropical montane cloud forests: science for conservation and management*. New York, USA: Cambridge University Press.

Bruijnzeel LA, Veneklaas EJ. 1998. Climatic conditions and tropical montane forest productivity: the fog has not lifted yet. *Ecology* **79**: 3–9.

von Caemmerer S, Evans JR, Hudson GS, Andrews TJ. 1994. The kinetics of ribulose-1, 5-bisphosphate carboxylase/oxygenase *in vivo* inferred from measurements of photosynthesis in leaves of transgenic tobacco. *Planta* **195**: 88–97.

Carswell FE, Meir P, Wandelli EV, Bonates LCM, Kruijt B, Barbosa EM, Nobre AD, Grace J, Jarvis PG. 2000. Photosynthetic capacity in a central Amazonian rain forest. *Tree Physiology* **20**: 179–186.

Cordell S, Goldstein G, Meinzer FC, Handley LL. 1999. Allocation of nitrogen and carbon in leaves of *Metrosideros polymorpha* regulates carboxylation capacity and $\delta^{13}C$ along an altitudinal gradient. *Functional Ecology* **13**: 811–818.

Coste S, Roggy J-C, Imbert P, Born C, Bonal D, Dreyer E. 2005. Leaf photosynthetic traits of 14 tropical rain forest species in relation to leaf nitrogen concentration and shade tolerance. *Tree Physiology* **25**: 1127–1137.

Domingues TF, Berry JA, Martinelli LA, Ometto JPHB, Ehleringer JR. 2005. Parameterization of canopy structure and leaf-level gas exchange for an eastern Amazonian tropical rain forest (Tapajós National Forest, Pará, Brazil). *Earth Interactions* **9**: 1–23.

Domingues TF, Ishida FY, Feldpausch T, Grace J, Meir P, Saiz G, Sene O, Schrodt F, Sonké B, Taedoumg H *et al.* 2015. Biome-specific effects of nitrogen and phosphorus on the photosynthetic characteristics of trees at a forest-savanna boundary in Cameroon. *Oecologia* **178**: 659–672.

Domingues TF, Martinelli LA, Ehleringer JR. 2007. Ecophysiological traits of plant functional groups in forest and pasture ecosystems from eastern Amazônia, Brazil. *Plant Ecology* **193**: 101–112.

Domingues TF, Meir P, Feldpausch TR, Saiz G, Veenendaal EM, Schrodt F, Bird M, Djagbletey G, Hien F, Compaore H *et al.* 2010. Co-limitation of photosynthetic capacity by nitrogen and phosphorus in West Africa woodlands. *Plant, Cell & Environment* **33**: 959–980.

Dusenge M, Wallin G, Gårdesten J, Niyonzima F, Adolfsson L, Nsabimana D, Uddling J. 2015. Photosynthetic capacity of tropical montane tree species in relation to leaf nutrients, successional strategy and growth temperature. *Oecologia* **177**: 1183–1194.

Evans JR. 1989. Photosynthesis and nitrogen relationships in leaves of C_3 plants. *Oecologia* **78**: 9–19.

Evans JR, Seemann JR. 1989. *The allocation of protein nitrogen in the photosynthetic apparatus: costs, consequences, and control*. New York, USA: Alan R. Liss.

Falster DS, Warton DI, Wright IJ. 2006. *SMATR: Standardised major axis tests and routines, version 2.0*. [WWW document] URL https://github.com/dfalster/smatr/ [accessed 4 April 2015].

Farquhar GD, von Caemmerer S, Berry JA. 1980. A biochemical model of photosynthetic CO_2 assimilation in leaves of C_3 species. *Planta* **149**: 78–90.

Flexas J, Ribas-Carbó M, Diaz-Espejo A, Galmés J, Medrano H. 2008. Mesophyll conductance to CO_2: current knowledge and future prospects. *Plant, Cell & Environment* **31**: 602–621.

Fredeen AL, Rao IM, Terry N. 1989. Influence of phosphorus nutrition on growth and carbon partitioning in *Glycine max*. *Plant Physiology* **89**: 225–230.

Fyllas NM, Patiño S, Baker TR, Bielefeld Nardoto G, Martinelli LA, Quesada CA, Paiva R, Schwarz M, Horna V, Mercado LM *et al.* 2009. Basin-wide variations in foliar properties of Amazonian forest: phylogeny, soils and climate. *Biogeosciences* **6**: 2677–2708.

Gaspar MM, Ferreira RB, Chaves MM, Teixeira AR. 1997. Improved method for the extraction of proteins from *Eucalyptus* leaves. Application in leaf response to temperature. *Phytochemical Analysis* **8**: 279–285.

Gentry AH. 1988. Changes in plant community diversity and floristic composition on environmental and geographical gradients. *Annals of the Missouri Botanical Garden* **75**: 1–34.

Girardin CAJ, Espejob JES, Doughty CE, Huasco WH, Metcalfe DB, Durand-Baca L, Marthews TR, Aragao LE, Farfán-Rios W, García-Cabrera K. 2014a. Productivity and carbon allocation in a tropical montane cloud forest in the Peruvian Andes. *Plant Ecology & Diversity* **7**: 107–123.

Girardin CAJ, Farfan-Rios W, Garcia K, Feeley KJ, Jørgensen PM, Murakami AA, Cayola Pérez L, Seidel R, Paniagua N, Fuentes Claros AF *et al.* 2014b. Spatial patterns of above-ground structure, biomass and composition in a network of six Andean elevation transects. *Plant Ecology & Diversity* **7**: 161–171.

Girardin CAJ, Malhi Y, Aragao LE, Mamani M, Huaraca Huasco W, Durand L, Feeley KJ, Rapp J, Silva-Espejo JE, Silman M *et al.* 2010. Net primary productivity allocation and cycling of carbon along a tropical forest elevational transect in the Peruvian Andes. *Global Change Biology* **16**: 3176–3192.

Grubb PJ. 1977. Control of forest growth and distribution on wet tropical mountains: with special reference to mineral nutrition. *Annual Review of Ecology and Systematics* **8**: 83–107.

Güsewell S. 2004. N: P ratios in terrestrial plants: variation and functional significance. *New Phytologist* **164**: 243–266.

Harrison MT, Edwards EJ, Farquhar GD, Nicotra AB, Evans JR. 2009. Nitrogen in cell walls of sclerophyllous leaves accounts for little of the variation in photosynthetic nitrogen-use efficiency. *Plant, Cell & Environment* **32**: 259–270.

Hikosaka K. 2004. Interspecific difference in the photosynthesis–nitrogen relationship: patterns, physiological causes, and ecological importance. *Journal of Plant Research* **117**: 481–494.

Hikosaka K, Ishikawa K, Borjigidai A, Muller O, Onoda Y. 2006. Temperature acclimation of photosynthesis: mechanisms involved in the changes in temperature dependence of photosynthetic rate. *Journal of Experimental Botany* **57**: 291–302.

Hikosaka K, Nagamatsu D, Ishii HS, Hirose T. 2002. Photosynthesis–nitrogen relationships in species at different altitudes on Mount Kinabalu, Malaysia. *Ecological Research* **17**: 305–313.

Hikosaka K, Shigeno A. 2009. The role of Rubisco and cell walls in the interspecific variation in photosynthetic capacity. *Oecologia* **160**: 443–451.

Jacob J, Lawlor DW. 1992. Dependence of photosynthesis of sunflower and maize leaves on phosphate supply, ribulose-1,5-bisphosphate carboxylase oxygenase activity, and ribulose-1,5-bisphosphate pool size. *Plant Physiology* **98**: 801–807.

Jacob J, Lawlor DW. 1993. Extreme phosphate deficiency decreases the *in vivo* CO_2/O_2 specificity factor of Ribulose 1,5-Bisphosphate Carboxylase-Oxygenase in intact leaves of sunflower. *Journal of Experimental Botany* **44**: 1635–1641.

Kattge J, Knorr W, Raddatz T, Wirth C. 2009. Quantifying photosynthetic capacity and its relationship to leaf nitrogen content for global-scale terrestrial biosphere models. *Global Change Biology* **15**: 976–991.

Kraft NJB, Valencia R, Ackerly DD. 2008. Functional traits and niche-based tree community assembly in an Amazonian forest. *Science* **322**: 580–582.

Kumagai To, Ichie T, Yoshimura M, Yamashita M, Kenzo T, Saitoh TM, Ohashi M, Suzuki M, Koike T, Komatsu H. 2006. Modeling CO_2 exchange over a Bornean tropical rain forest using measured vertical and horizontal variations in leaf-level physiological parameters and leaf area densities. *Journal of Geophysical Research: Atmospheres* **111**: D10107.

Lauer MJ, Pallardy SG, Blevins DG, Randall DD. 1989. Whole leaf carbon exchange characteristics of phosphate deficient soybeans (*Glycine max* L.). *Plant Physiology* **91**: 848–854.

Letts MG, Mulligan M. 2005. The impact of light quality and leaf wetness on photosynthesis in north-west Andean tropical montane cloud forest. *Journal of Tropical Ecology* **21**: 549–557.

Lloyd J, Bloomfield K, Domingues TF, Farquhar GD. 2013. Photosynthetically relevant foliar traits correlating better on a mass vs an area basis: of ecophysiological relevance or just a case of mathematical imperatives and statistical quicksand? *New Phytologist* **199**: 311–321.

Loustau D, Brahim MB, Gaudillère J-P, Dreyer E. 1999. Photosynthetic responses to phosphorus nutrition in two-year-old maritime pine seedlings. *Tree Physiology* **19**: 707–715.

Malhi Y. 2010. The carbon balance of tropical forest regions, 1990–2005. *Current Opinion in Environmental Sustainability* **2**: 237–244.

Medlyn BE, Dreyer E, Ellsworth D, Forstreuter M, Harley PC, Kirschbaum MUF, Le Roux X, Montpied P, Strassemeyer J, Walcroft A *et al.* 2002. Temperature response of parameters of a biochemically based model of photosynthesis. II. A review of experimental data. *Plant, Cell & Environment* **25**: 1167–1179.

Meir P, Kruijt B, Broadmeadow M, Barbosa E, Kull O, Carswell F, Nobre A, Jarvis PG. 2002. Acclimation of photosynthetic capacity to irradiance in tree canopies in relation to leaf nitrogen concentration and leaf mass per unit area. *Plant, Cell & Environment* **25**: 343–357.

Meir P, Levy P, Grace J, Jarvis P. 2007. Photosynthetic parameters from two contrasting woody vegetation types in West Africa. *Plant Ecology* **192**: 277–287.

Mercado LM, Patiño S, Domingues TF, Fyllas NM, Weedon GP, Sitch S, Quesada CA, Phillips OL, Aragao LE, Malhi Y *et al.* 2011. Variations in Amazon forest productivity correlated with foliar nutrients and modelled rates of photosynthetic carbon supply. *Philosophical Transactions of the Royal Society B: Biological Sciences* **366**: 3316–3329.

Niinemets Ü, Tenhunen JD. 1997. A model separating leaf structural and physiological effects on carbon gain along light gradients for the shade-tolerant species *Acer saccharum*. *Plant, Cell & Environment* **20**: 845–866.

Pinheiro J, Bates D. 2000. *Mixed-effects models in S and S-PLUS*. New York, USA: Springer.

Pons TL, van der Werf A, Lambers H. 1994. *Photosynthetic nitrogen use efficiency of inherently low- and fast-growing species: possible explanations for observed differences*. The Hague, the Netherlands: SPB Academic Publishing.

Poorter H, Evans JR. 1998. Photosynthetic nitrogen-use efficiency of species that differ inherently in specific leaf area. *Oecologia* **116**: 26–37.

Quesada CA, Lloyd J, Schwarz M, Patiño S, Baker TR, Czimczik C, Fyllas NM, Martinelli L, Nardoto GB, Schmerler J *et al.* 2010. Variations in chemical and physical properties of Amazon forest soils in relation to their genesis. *Biogeosciences* 7: 1515–1541.

Quesada CA, Phillips OL, Schwarz M, Czimczik CI, Baker TR, Patiño S, Fyllas NM, Hodnett MG, Herrera R, Almeida S *et al.* 2012. Basin-wide variations in Amazon forest structure and function are mediated by both soils and climate. *Biogeosciences* **9**: 2203–2246.

Quilici A, Medina E. 1998. Photosynthesis-nitrogen relationships in pioneer plants of disturbed tropical montane forest sites. *Photosynthetica* **35**: 525–534.

R Development Core Team 2011. *R: a language and environment for statistical computing*. [WWW document] URL http://www.R-project.org/. Vienna, Austria: The R Foundation for Statistical Computing.

Raaimakers D, Boot RGA, Dijkstra P, Pot S. 1995. Photosynthetic rates in relation to leaf phosphorus content in pioneer versus climax tropical rainforest trees. *Oecologia* **102**: 120–125.

Rada F, García-Núñez C, Ataroff M. 2009. Leaf gas exchange in canopy species of a Venezuelan cloud forest. *Biotropica* **41**: 659–664.

Reich P, Oleksyn J, Wright I. 2009. Leaf phosphorus influences the photosynthesis–nitrogen relation: a cross-biome analysis of 314 species. *Oecologia* **160**: 207–212.

Reich PB, Walters MB. 1994. Photosynthesis-nitrogen relations in Amazonian tree species. *Oecologia* **97**: 73–81.

Sage RF, Kubien DS. 2007. The temperature response of C_3 and C_4 photosynthesis. *Plant, Cell & Environment* **30**: 1086–1106.

Santiago LS, Mulkey SS. 2003. A test of gas exchange measurements on excised canopy branches of ten tropical tree species. *Photosynthetica* **41**: 343–347.

Silman MR. 2014. Functional megadiversity. *Proceedings of the National Academy of Sciences, USA* **111**: 5763–5764.

Stitt M, Schulze D. 1994. Does Rubisco control the rate of photosynthesis and plant growth? An exercise in molecular ecophysiology. *Plant, Cell & Environment* **17**: 465–487.

Takashima T, Hikosaka K, Hirose T. 2004. Photosynthesis or persistence: nitrogen allocation in leaves of evergreen and deciduous *Quercus* species. *Plant, Cell & Environment* **27**: 1047–1054.

Tanner E, Vitousek PM, Cuevas E. 1998. Experimental investigation of nutrient limitation of forest growth on wet tropical mountains. *Ecology* **79**: 10–22.

Terashima I, Masuzawa T, Ohba H, Yokoi Y. 1995. Is photosynthesis suppressed at higher elevations due to low CO_2 pressure? *Ecology* **76**: 2663–2668.

Townsend AR, Cleveland CC, Asner GP, Bustamante MMC. 2007. Controls over foliar N: P ratios in tropical rain forests. *Ecology* **88**: 107–118.

Vårhammar A, Wallin G, McLean CM, Dusenge ME, Medlyn BE, Hasper TB, Nsabimana D, Uddling J. 2015. Photosynthetic temperature responses of tree species in Rwanda: evidence of pronounced negative effects of high temperature in montane rainforest climax species. *New Phytologist* **206**: 1000–1012.

Vitousek PM. 1984. Litterfall, nutrient cycling, and nutrient limitation in tropical forests. *Ecology* **65**: 285–298.

Walker AP, Beckerman AP, Gu LH, Kattge J, Cernusak LA, Domingues TF, Scales JC, Wohlfahrt G, Wullschleger SD, Woodward FI. 2014. The relationship of leaf photosynthetic traits - V_{cmax} and J_{max} - to leaf nitrogen, leaf phosphorus, and specific leaf area: a meta-analysis and modeling study. *Ecology and Evolution* **4**: 3218–3235.

Warren CR, Adams MA. 2001. Distribution of N, Rubisco and photosynthesis in *Pinus pinaster* and acclimation to light. *Plant, Cell & Environment* **24**: 597–609.

Warren CR, Adams MA. 2002. Phosphorus affects growth and partitioning of nitrogen to Rubisco in *Pinus pinaster*. *Tree Physiology* **22**: 11–19.

Warren CR, Adams MA, Chen Z. 2000. Is photosynthesis related to concentrations of nitrogen and Rubisco in leaves of Australian native plants? *Functional Plant Biology* **27**: 407–416.

Warton DI, Wright IJ, Falster DS, Westoby M. 2006. Bivariate line-fitting methods for allometry. *Biological Reviews* **81**: 259–291.

van de Weg M, Meir P, Grace J, Atkin OK. 2009. Altitudinal variation in leaf mass per unit area, leaf tissue density and foliar nitrogen and phosphorus content along an Amazon-Andes gradient in Peru. *Plant Ecology & Diversity* **2**: 243–254.

van de Weg M, Meir P, Grace J, Ramos G. 2012. Photosynthetic parameters, dark respiration and leaf traits in the canopy of a Peruvian tropical montane cloud forest. *Oecologia* **168**: 23–34.

van de Weg M, Meir P, Williams M, Girardin C, Malhi Y, Silva-Espejo J, Grace J. 2014. Gross primary productivity of a high elevation tropical montane cloud forest. *Ecosystems* **17**: 751–764.

Westbeek MHM, Pons TL, Cambridge ML, Atkin OK. 1999. Analysis of differences in photosynthetic nitrogen use efficiency of alpine and lowland *Poa* species. *Oecologia* **120**: 19–26.

Wittich B, Horna V, Homeier J, Leuschner C. 2012. Altitudinal change in the photosynthetic capacity of tropical trees: a case study from Ecuador and a pantropical literature analysis. *Ecosystems* **15**: 958–973.

Wright IJ, Reich PB, Westoby M, Ackerly DD, Baruch Z, Bongers F, Cavender-Bares J, Chapin T, Cornelissen JHC, Diemer M *et al.* 2004. The worldwide leaf economics spectrum. *Nature* **428**: 821–827.

Wullschleger SD. 1993. Biochemical limitations to carbon assimilation in C_3 plants – a retrospective nalysis of the A/C_i curves from 109 species. *Journal of Experimental Botany* **44**: 907–920.

Zuur A, Ieno EN, Walker N, Saveliev AA, Smith GM. 2009. *Mixed effects models and extensions in ecology with R.* Berlin and Heidelberg, Germany: Springer.

Supporting Information

Additional Supporting Information may be found online in the Supporting Information tab for this article:

Fig. S1 Plots of photosynthetic parameters against mean annual temperature and soil [P] for each site.

Fig. S2 Plots of % n_P, % n_R, and % n_E, in relation to M_a, N_a, and P_a.

Fig. S3 Plots of the fraction of leaf N allocated to Rubisco, n_R, in relation to leaf mass per unit leaf area, M_a.

Fig. S4 Stacked graph showing n_E, n_P and n_R (*in vivo* and *in vitro*) for individual leaves.

Fig. S5 Plots for linear mixed-effects model goodness of fits, including fixed and random terms for $V_{cmax,a}{}^{25}$ and $J_{max,a}{}^{25}$.

Table S1 Summary of species sampled at each site and their parameters

Table S2 Pearson correlations for bivariate relationships among leaf traits and environmental parameters

Table S3 Standardized major axis regression slopes for relationships in Figs 2, 4, 5 and 6

Table S4 Means ± SD of leaf physiology and chemistry, expressed on an area basis for each site

Table S5 Standardized major axis regression slopes for relationships in Figs 8 and S2

Table S6 Stepwise selection process for the fixed component of the linear mixed effect model to determine the best predictive model given in Table 3

Table S7 Mean values of $V_{cmax,a}{}^{25}$ and $J_{max,a}{}^{25}$ in upland and lowland plants calculated using different activation energies for each parameter

Methods S1 Additional study site details.

Methods S2 Identification of outliers and $A \leftrightarrow C_i$ curve methodological details.

Methods S3 Optimization of protocols for protein extraction from the leaves of recalcitrant tree species.

Please note: Wiley Blackwell are not responsible for the content or functionality of any supporting information supplied by the authors. Any queries (other than missing material) should be directed to the *New Phytologist* Central Office.